AD NUMBER

ADB160619

NEW LIMITATION CHANGE

TO

Approved for public release, distribution unlimited

FROM

Distribution authorized to DoD only; Proprietary Information; Oct 1990. Other requests shall be referred to USAMRDC, Attn: SGRD-RMI-S, Fort Detrick, Frederick, MD 21702-5012.

AUTHORITY

Per SGRD-RMI-S ltr dtd 4 Mar 1994.

AD _____

CONTRACT NO: DAMD17-90-C-0086

TITLE: Broadband Near IR Laser Hazard Filters

INVESTIGATOR: Gajendra Savant, Ph.D.

CONTRACTING ORGANIZATION: Physical Optics Corporation
20600 Gramercy Place, Suite 103
Torrance, CA 90501

REPORT DATE: October 2, 1990

TYPE OF REPORT: Final, Phase I

PREPARED FOR: U.S. ARMY MEDICAL RESEARCH AND DEVELOPMENT COMMAND, Fort Detrick, Frederick, Maryland 21702-5012

REPORT DOCUMENTATION PAGE

Form Approved
OMB No. 0704-0188

1. AGENCY USE ONLY (Leave blank)	2. REPORT DATE	3. REPORT TYPE AND DATES COVERED
	October 2, 1990	Final, Phase I 2 Apr 90-2 Oct 90

4. TITLE AND SUBTITLE
Broadband Near IR Laser Hazard Filters

5. FUNDING NUMBERS
DAMD17-90-C-0086

6. AUTHOR(S)
Gajendra Savant, Ph.D.

7. PERFORMING ORGANIZATION NAME(S) AND ADDRESS(ES)
Physcial Optics Corporation
20600 Gramercy Place, Suite 103
Torrance, CA 90501

8. PERFORMING ORGANIZATION REPORT NUMBER

9. SPONSORING/MONITORING AGENCY NAME(S) AND ADDRESS(ES)
U.S. Army Medical Research and Development Command
Fort Detrick, Frederick, MD 21702-5012

10. SPONSORING/MONITORING AGENCY REPORT NUMBER

11. SUPPLEMENTARY NOTES

12a. DISTRIBUTION/AVAILABILITY STATEMENT
"Distribution authorized to DOD Components only, ~~under specific authority of the Small Business Innovation Development Act of 1982, P.L. 97-219 and 10 USC 2320~~ (October 1990). Other requests shall be referred to the USAMRDC, ATTN: SGRD-RMI-S, Fort Detrick, Frederick, MD 21702-5012

12b. DISTRIBUTION CODE

13. ABSTRACT (Maximum 200 words)

PROPRIETARY INFORMATION

14. SUBJECT TERMS
Laser, Hazards

15. NUMBER OF PAGES
55

16. PRICE CODE

17. SECURITY CLASSIFICATION OF REPORT	18. SECURITY CLASSIFICATION OF THIS PAGE	19. SECURITY CLASSIFICATION OF ABSTRACT	20. LIMITATION OF ABSTRACT
Unclassified	Unclassified		

Sponsored By: The U.S. Army Medical Research and Development Command

BROADBAND NEAR IR LASER HAZARD FILTERS

Contract No. DAMD17-90-C-0086
Period of Performance: 04-02-90 through 10-02-90

FINAL REPORT

October 2, 1990

Sequence Number "FINAL"

Reporting Period: 04-02-90 through 10-02-90

Presented To:

U.S. Army Medical Research Acquisition Activity
Fort Detrick
Frederick, Maryland 21701-5014

Contracting Officer: Mr. Craig D. Lebo
(301) 695-2800

Technical Monitor: Mr. Jack Lund
(415) 561-4367

Prepared by:

Gajendra Savant Ph.D.
Principal Investigator

Physical Optics Corporation
20600 Gramercy Place, Suite 103
Torrance, California 90501
(213) 320-3088

TABLE OF CONTENTS

ABSTRACT

Physical Optics Corporation (POC) investigated the fabrication of holographic broadband laser eye protection (BLEP) filters as a new approach to protecting ground troops from eye damage by near infrared (IR) lasers. The infrared broadband filters investigated during the Phase I research program combined high optical density (OD > 4), high photopic visual transmission efficiency (60 to 75%) and large angular protection (> 40°) for the 694 nm wavelength and with the environmental stability necessary for battlefield conditions. During its Phase I research, POC successfully fabricated broadband IR filters with excellent optical qualities. In addition, BLEP filters are compatible with flat and curved polycarbonate substrates and can be combined with absorption dye technology to yield cost effective hybrid technology for laser eyewear.

This technology should be able to supply complete wavelength and angular laser protection for the near IR portion of the spectrum from 690 nm to 1100 nm for the Army's spectacle, goggle or visor configurations with appropriate OD and photopic efficiency. Further research is needed to extend this technology to contain hybrid scenarios on the various substrates noted above.

The benefits to the Tri-Service Agencies are that protection against all agile laser threats in the 690 nm to 1100 nm region will be developed. Commercial applications of this broadband near IR rejection filter technology are to automotive and architectural window glass coating for the reduction of cooling loads. In addition to eye protection, BLEP filters can be used for cockpit display filters, for night vision goggles, for broadband IR reflectors for space solar cell arrays, and perhaps even for very large (greater than 1 m^2) near IR optical mirrors.

1.0 IDENTIFICATION AND SIGNIFICANCE OF THE PROBLEM

Highly-efficient broadband laser eye protection (BLEP) filters were investigated in Phase I by Physical Optics Corporation (POC) as a new approach for protecting ground troops from eye damage by frequency agile near infrared (IR) lasers. The broadband filters prevent the transmission of concentrated light energy that causes thermal burns to the retina. These filters will combine high optical density, high photopic visual transmission and large angular protection with the ruggedness and the environmental stability necessary for battlefield conditions. In addition, these BLEP filters have shown high laser damage threshold (4 GW/cm^2), required temperature stability, reproducibility and a promise of low cost in mass production.

In order to provide the Army's requirements for ocular and system protection in the near IR region (690 nm to 1100 nm), a filter should have for the following properties:

(a) Ballistic protection
(b) High optical density
(c) Abrasion resistance
(d) High photopic and scotopic luminous transmission
(e) Minimum haze
(f) Broadband protection for frequency agile near IR laser threats
(g) Survivability under harsh conditions such as temperature, salt spray, and humidity

Based on volume holography and advanced holographic recording materials, POC's BLEP filters have shown promise for simultaneously fulfilling these requirements. During the Phase I research, POC theoretically and experimentally investigated the performance and advantages of broadband IR holographic filters. As a result of our research, we have identified optimum designs and optimum synthesis and processing conditions under which to produce these filters. POC's approach has several material and process engineering advantages over the dielectric multilayer approach; the most important of those advantages appears to be cost.

POC is currently developing methods that allow for the incorporation of these holographic filters in sandwich-type active $\chi^{(2)}$ structures which would result in agile laser protection for the visible portion of the spectrum. In this sandwich-type structure, the holograms are separated by a $\chi^{(2)}$ nonlinear optical material which is fast-switching (on the order of 1 psec). With this added layer, a tunable filter can be fabricated which can be either transmissive or highly reflective (depending upon whether the filter is under attack).

1.1 Review of Existing Technology

Existing laser eye protection uses absorption dyes in glass or polycarbonate spectacles, goggles or plastic visors in order to absorb a broad range of near IR laser radiation. However, absorption dyes can only be applied to one (or possibly two) line(s) in the visible portion of the spectrum and still maintain acceptable photopic/scotopic efficiencies. Although their absorption bandwidths are generally broad, their photopic/scotopic efficiencies are typically less than 20% for multiwavelength protection (2 wavelengths in the visible) and the long-term lifetime of dyes exposed to sunlight continues to be a question mark. Setting aside the difficult problem of dealing with the increased number of laser threat wavelengths in the visible portion of the spectrum, a satisfactory solution must still be found for protection against all agile threats in the near IR portion of the spectrum.

Nonlinear optical materials currently require a focal plane to obtain the required intensity levels for switching and, therefore, are not serious candidates for foot soldier laser eyewear. In general, nonlinear materials need a high threshold of incident light before they switch, thereby severely impairing their effectiveness against low power (milliwatt) laser threats. Nonlinear materials are generally expensive to produce and, thus, the weight, size, and complexity of such systems also hamper their widespread use for laser hardening applications.

Glasses such as the Schott Optical Glass BG-39 provide absorption protection from the red end of the visible spectrum (out to about 1.2 μm). However, when ballistic protection is required in addition to laser eye protection, a polycarbonate visor or goggle is the preferred approach.

Interference filters can be made to cover laser threat lines for the near IR portion of the spectrum. While these filters can be fabricated using vacuum deposition of multilayer dielectric stacks, usually about 200 layers are required at a cost of about $200/filter. However, multilayers are extremely difficult to achieve in mass production, especially for large sizes (> 1 ft^2). On the other hand, a very large number of periods (> 300) is no problem for the holographic case. The other fundamental advantage of holographic structures over multilayers is that they do not need to be limited to the Lippmann case for eye-centered recording geometries. POC projects the cost of holographic broadband near IR filters to be 1/3 to 1/4 the cost of equivalent dielectric multilayer filters and, in addition, the holographic filters can achieve much higher OD.

2.0 SUMMARY OF PHASE I RESULTS

In this section of the report, we will summarize the results of our Phase I research program.

2.1 Phase I Technical Objectives and Achievements

The purpose of the Phase I research was to demonstrate the feasibility of fabricating and studying the environmental stability of broadband holographic filters with an optical density greater than 3, an optical bandwidth of 450 nm, a cut-on wavelength of 690 nm, a cut-off wavelength of 1120 nm, and a photopic efficiency of 75%. In order to do so, we concurrently pursued the following three objectives:

1. To determine the optimum holographic recording emulsion based on an organic polymer, a sensitizer, an electron-donating additive, variations in the solution viscosity and pH, the exposure and processing conditions, and the coating thickness.

2. To experimentally demonstrate the fabrication of a broadband filter with optical density greater than 3, bandwidth of 400-450 nm and approximately 75% photopic/scotopic efficiency.

3. To evaluate the performance of BLEP filters as an environmentally- and thermally-stable near IR protection system.

In order to demonstrate the feasibility of fabricating efficient holographic filters for near IR radiation, we conducted a theoretical and experimental investigation of material optimization, optimum optical recording design, processing conditions, substrates and encapsulation using various optical adhesives. This involved the successful development of an IR-sensitive recording material. Thus, POC addressed all of the work tasks listed in its Phase I proposal to Fort Detrick. The major achievements of this program are summarized below.

1. *Theoretical Studies and Analysis*
   Theoretical studies and analysis proved that the filter was efficient in reflecting incoming radiation over a broad spectral range. In order to evaluate the influence of absorption and scattering losses on the diffraction efficiency in the IR region,

Kogelnik's model of fully-uniform lossy gratings was adopted. Based on the results from this analysis, one can design the desired broadband laser eye protection filter for near IR regions.

2. *Design and Fabrication of the BLEP Filters*

Fabrication technology for BLEP filters was successfully developed. Two designs for obtaining high-efficiency broadband IR filters were investigated. One was based on the new red-sensitive holographic recording medium (sensitive to a 633 nm HeNe laser) and the other was based on a recording medium that is sensitive to a 512 nm green laser. The recording setups are illustrated in Figures 2-1 and 2-2, respectively. Phase II fabrication will involve the down selecting of one of these two methods. Details of the exposure methods and attributes of each method are discussed in Section 4.4.

3. *Development and Optimization of the Holographic Recording Media*

A volume holographic recording medium sensitive to red wavelengths was developed. The material development effort involved a detailed understanding of the chemistry of the medium including solution pH, viscosity, sensitizer concentration, sensitivity, the role of the electron donor as a sensitivity enhancer and shelf life of the media. Thus, we successfully optimized a new holographic recording medium that is sensitive to the 632 nm laser wavelength. As a result of this optimization, we were able to obtain bandwidths of 100-400 nm with acceptable OD values.

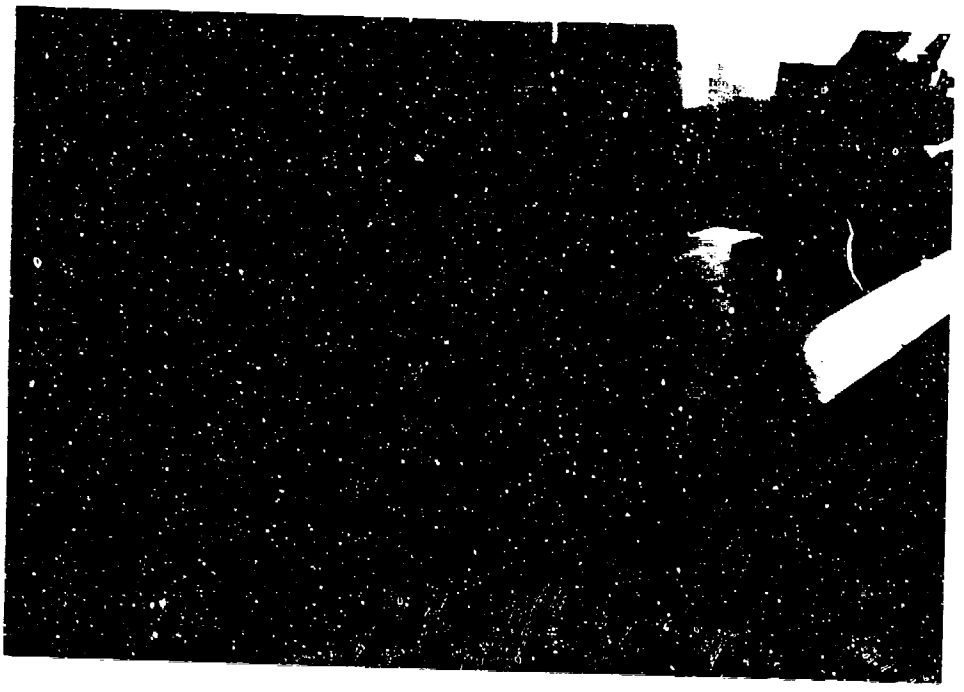

Figure 2-1 Fabrication and Exposure Setup for POC's BLEP Filters Using a HeNe Laser.

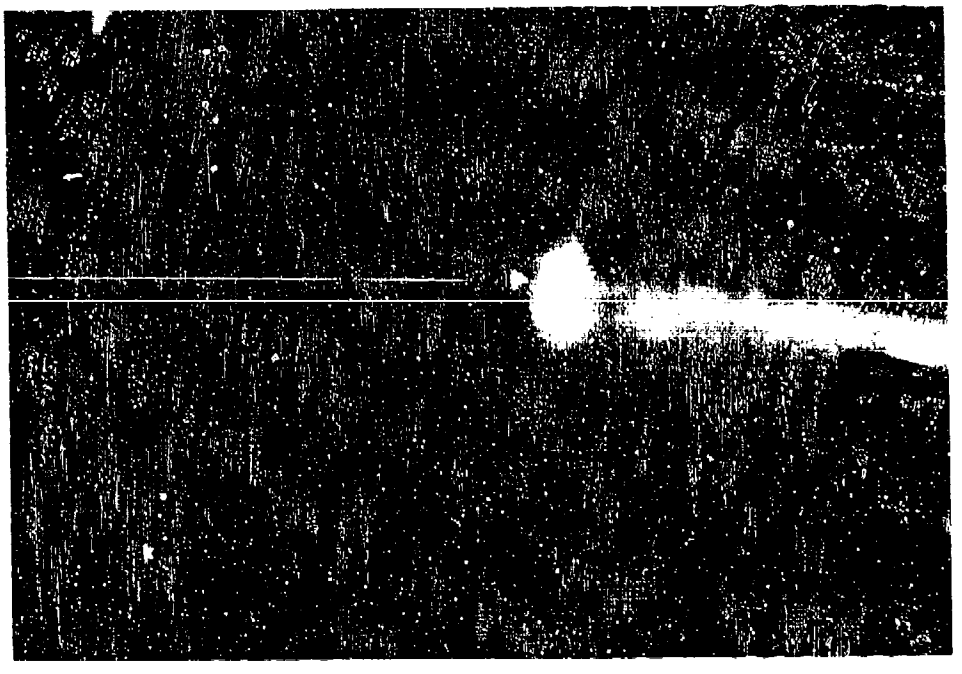

Figure 2-2 Fabrication and Exposure Setup for POC's BLEP Filters Using an Ar^+ Ion Laser.

4. *Processing*

A new processing technology appropriate to this new holographic recording medium was successfully developed. These processing techniques helped tune the filters to the desired peak wavelength and bandwidth. In addition, these processing techniques enhanced the optical density and reduced the noise and absorption. Details of the processing technique are discussed in Section 3.

5. *Selection of the Substrate*

The IR filter was successfully coated onto transparent glass substrates, glass mirrors and plastic substrates. The plastic substrates used in Phase I were polycarbonate, PMMA, Mylar, TPX, and Aclar. POC's holographic coating was also successfully placed on curved and flexible substrates.

6. *Lamination and Encapsulation*

The moisture barrier coatings and encapsulation technology were developed to protect the broadband laser eye protection filters from moisture and abrasion. Thus far, POC has tested a number of UV-curable, thermally-stable and transparent adhesives compatible with the holographic recording material used in the BLEP filter fabrication and found Norland #61 and Master Bond UV-15 to be the best adhesives for lamination. Other adhesives currently under investigation include two-part epoxies UV-15-7, UV-15-75P4, UV-10 and EP-30 by Master Bond and other thermally-curable adhesives available on the market.

7. *Environmental Stability Test*

POC's recently developed broadband IR filters were successfully tested for

(a) high temperature stability without lamination
(b) high temperature cycling at 135°C without lamination
(c) prolonged duration with lamination in boiling water
(d) laser damage threshold test at shorter wavelengths with lamination
(e) simultaneous pressure and temperature without lamination
(f) water immersion at 52°C with lamination

8. *Optical Performance of the BLEP Filter*

We successfully evaluated most of the broadband IR filters for their optical density, bandwidth, angular acceptance, absorption, transmission, scattering, etc.

The theoretical, analytical and experimental Phase I results support POC's belief in the applicability of holographic broadband near IR filters. In addition, the material used in the filter fabrication is fully compatible with other materials used for visible laser eye protection devices including dielectric multilayers, absorption dyes and polycarbonate substrates. In order to advance the holographic broadband protection filter technology to the point where BLEP filters can be routinely mass produced, further efforts to refine the fabrication process, processing technology, including lamination and encapsulation, are still needed.

2.2 Theoretical Model for BLEP Filters

The first theoretical model describing the optical properties of broadband holographic filters was proposed by Tomasz Jannson--one of the key POC personnel for this program--based on the WKB method, analogous to that used in quantum mechanics. Such filters represent non-uniform Lippmann-Bragg holographic structures with grating constants which are chirped normal to the surface (see Figure 2-3).

Denoting the grating period by Λ and the normal coordinate by z, we can write

$$\Lambda = \Lambda(z) \tag{2-1}$$

Such a non-uniform structure produces enlarged spectral bandwidth $\Delta\lambda$ which is determined by the following basic formula,

$$\frac{\Delta\lambda}{\bar{\lambda}_B} = \frac{\Delta n}{\bar{n}} + \frac{\Delta\Lambda}{\bar{\Lambda}} \tag{2-2}$$

where λ_B is average Bragg wavelength, Δn-index modulation, $\bar{n}$-average refractive index, $\Delta\Lambda$-grating period change, and $\bar{\Lambda}$ - average grating period.

For $\Delta\Lambda = 0$, we obtain the uniform case (see, Figure 2-3(a)). It should be noted that Eq. (2-2) is approximate and holds only for moderate non-uniformities when the remaining parameters of the hologram (average refractive index and index modulation) remain constant. Such a situation is illustrated in Figure 2-4. In practice, Eq. (2-2) is a very useful approximation for evaluation purposes.

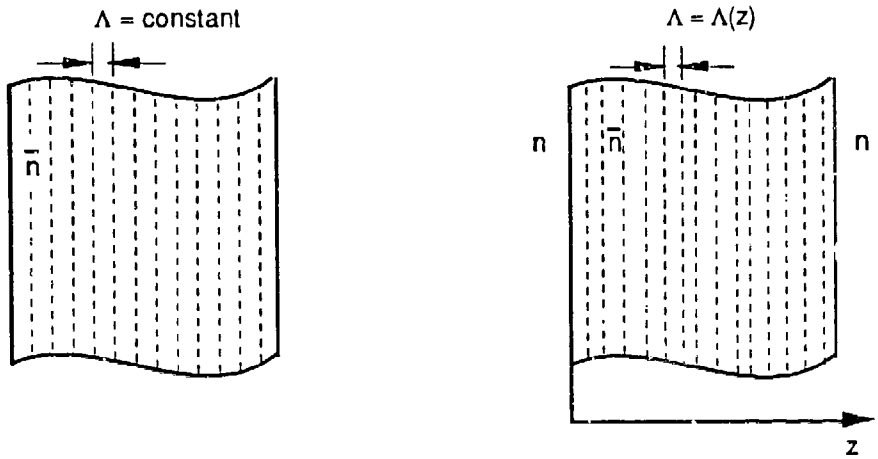

(a) (b)

Figure 2-3 Grating period distribution for Lippmann-Bragg holographic filters, assuming a) uniform distribution, b) non-uniform distribution.

A new and more accurate theory and computer software for Lippmann-Bragg broadband holographic filters have recently been developed at POC. This new model is based on the multiple-beam interference method and Kogelnik's local solution for uniform gratings (also called the method of effective interfaces). POC's computer method based on this model is orders of magnitude faster and more accurate than the matrix method (used in multilayer theory) where a large number of homogeneous slabs have to be used.

In order to show the effectiveness of POC's approach, let us consider a thick grating with a large number of periods, N. The number N can be determined from the following formula:

$$N = \frac{T}{\bar{\Lambda}} = \frac{2\bar{n}T}{\bar{\lambda}_B} \qquad (2\text{-}3)$$

where T is the hologram thickness. Figure 2-5 illustrates the theoretical hologram reflectance for T = 88 μ, and $\bar{\lambda}_B$ = 0.8 μ. Thus, for $\bar{n}$ = 1.55, we have a filter with N = 343 layers as calculated from equation (2.3).

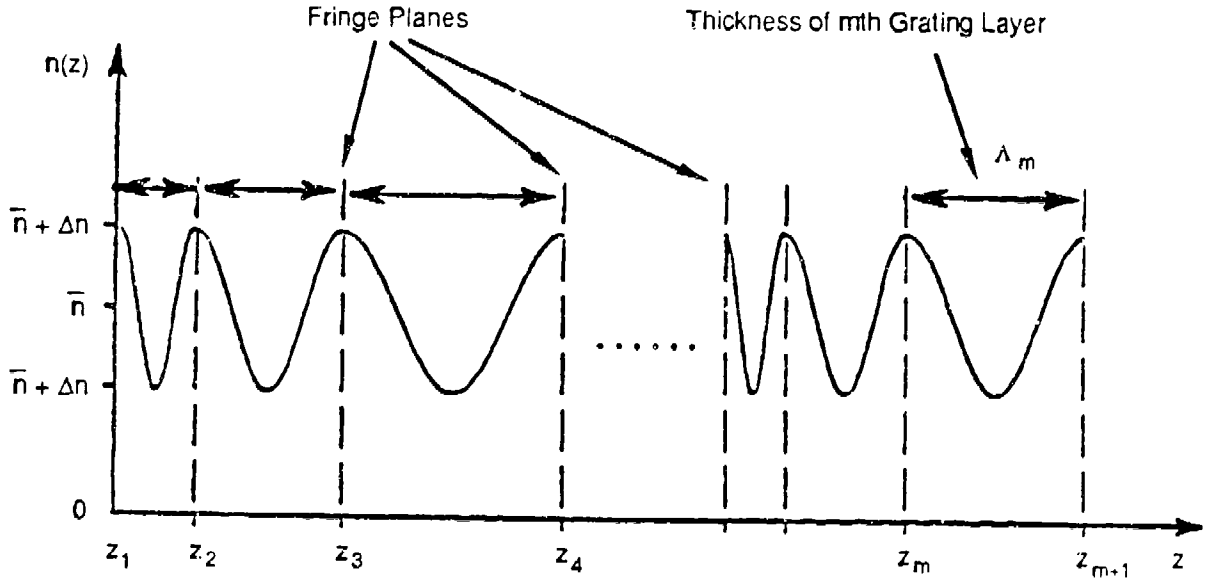

Figure 2-4 Illustration of Non-Uniform Distribution of Grating Period Λ.

The basic numerical results for efficiency and bandwidth of non-uniform holographic structures are illustrated in Figure 2-6. They have been demonstrated for a broad variety of grating non-uniformities ($\Delta\Lambda/\bar{\Lambda}$ = 0.05, 0.1, and 0.2), and index modulations ($0.01 < \Delta n < 0.2$), and for standard hologram thickness (T = 20 μm). The hologram bandwidth analysis demonstrates that in order to obtain high O.D. within the broad spectral range (> 300 nm), both high grating non-uniformity and high index modulation are necessary. On the other hand, it should be noted that parameters $\Delta\Lambda/\Lambda$, and Δn should be properly balanced in order to obtain broad flat bandwidth. Compare Figures 2-6 and 2-7 to see this striking result.

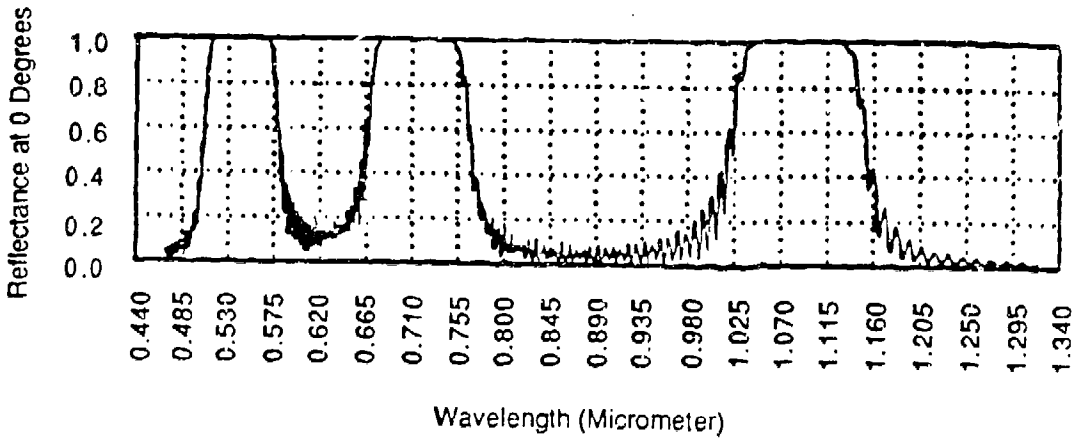

Figure 2-5 Illustration of the throughput calculated by POC's method of effective interfaces. Here, this method has been tested for N = 369 and three different period distributions located at the same hologram (T = 88 μm, Δn = 0.1, $\bar{n}$ = 1.56).

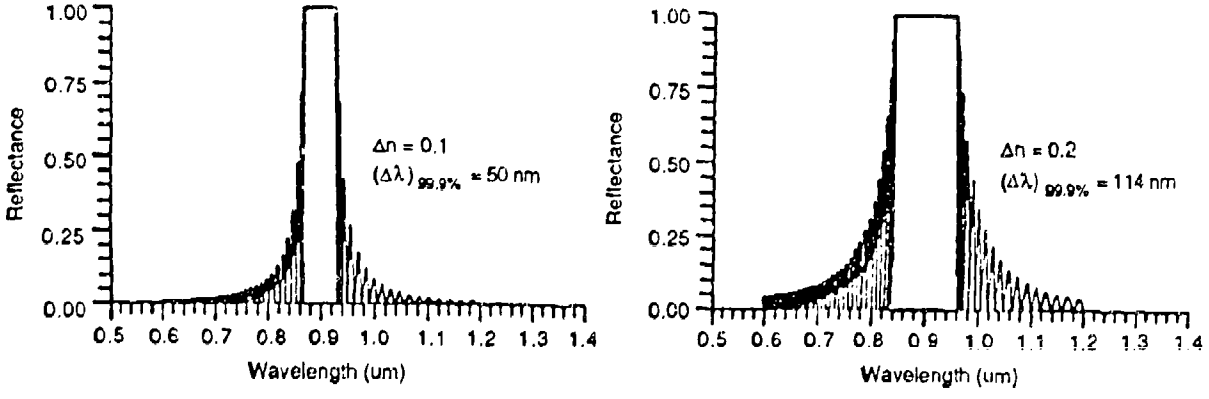

(a) (b)

Figure 2-6 Reflectance for the uniform hologram ($\frac{\Delta\Lambda}{\Lambda}$ = 0), for λ_B = 900 nm, n = 1.55, T = 20 μm, including: (a) Δn = 0.1, (b) Δn = 0.2.

The above theoretical results coincide with POC's experimental data obtained earlier for broadband solar-control windows.

The other important result is that, despite large grating period nonuniformities, the holograms are free of 2nd and higher order harmonics. This is due to the sinusoidal profile of the refractive index modulation which is locally preserved within the hologram thickness. The accuracy of this conclusion has been double-checked by the matrix method. In practice, controlling harmonics is difficult and requires sophisticated processing technology. However, POC believes that it is possible to develop full control of this technology from the fabrication standpoint and this will be demonstrated in the Phase II program.

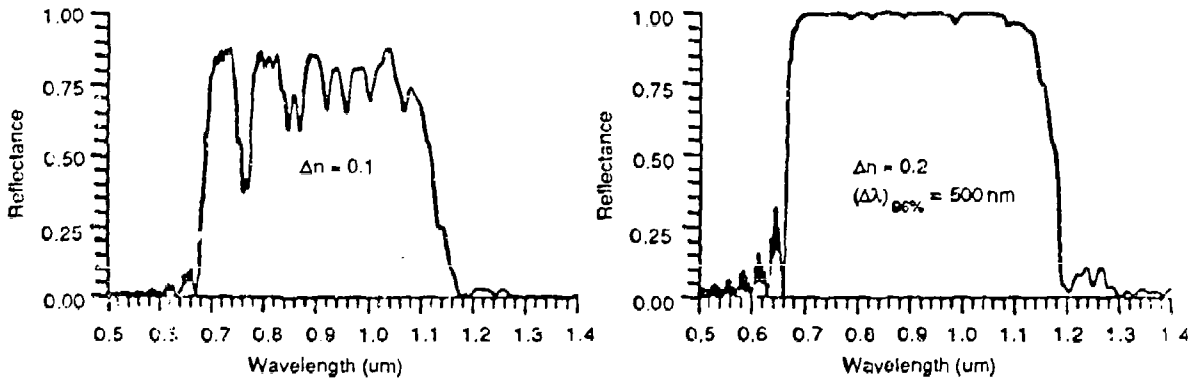

(a) (b)

Figure 2-7 Reflectance for the nonuniform hologram ($\frac{\Delta\Lambda}{\Lambda} = 0.1$) and the same remaining parameters as in Figure 2-6.

3.0 TECHNICAL DISCUSSION

Previous efforts to adapt a high-efficiency holographic technology based on dichromated gelatin (DCG) material to the near IR spectrum were limited by the size of the bandwidth and the moisture barrier encapsulation. Other results [1-8] related to near IR filters have been limited to dielectric multilayers with costs almost prohibitive for Army laser protective eyewear. In order to overcome these limitations, we have formulated new holographic materials (DPX-1 and IRT-6) which yield high-performance IR filters throughout the near IR region (from 600 nm to 2.7 μm). In the following subsections, we will describe the material studies for formulating DPX-1 and IRT-6, the

optical characteristics of BLEP filters such as optical density, angular protection and bandwidths, absorption dye broadband protection and field deployment requirements. We will also discuss the feasibility of mass producing BLEP filters on polycarbonate-substrates which includes encapsulation/lamination using commercially-available optical adhesives. Environmental survivability tests, including temperature cycling, laser damage, sunlight exposure, salt spray, humidity, etc., will also be considered.

3.1 POC's Advanced Material Technology

The success or failure of modern optical devices and systems depends to a great extent on the performance and survivability of the optical materials which are used. This is especially true for volume holographic structure-based filters, mirrors, switches and countermeasures. Unlike dielectric multilayer structures where multiple steps are required to fabricate a single multilayer structure, multiple holographic Bragg planes can be created in a single step in the bulk of the coating. As a result, volume holography offers great advantages unequaled by any other optical technology currently available to the Army in the areas of laser hardening and eye protection.

The general demands holography makes on recording materials involve (i) resolution, (ii) sensitivity, (iii) low noise and recording linearity, (iv) processibility and (v) stability. In recent times there have been major advances in volume holographic materials which can accommodate these requirements. A long list of major holographic materials includes silver halide films, photopolymers (DuPont, Polaroid's DMP-128, PVK), DCG, photochromics and ferroelectric crystals. As a result of the materials' availability, applications such as laser hardening, solar control IR mirrors, UV mirrors and other holographic optical elements should now be possible to fabricate at modest cost. In these applications, intense (> 10 W) and stable Argon ion laser sources are used for holographic recording in visible light-sensitive material. Although Bragg shift can be achieved by appropriate recording geometries and chemical processing, the visible light sources and visible light-sensitive materials are generally less effective and more expensive for routine production of laser hardening devices in the near IR region. Therefore, POC initiated a broad investigation of near IR holographic recording material development in Phase I of this program. As a result of material development efforts over the last several years, in general, and over the last six months, in particular, POC's material show great promise for mass production of laser protection eyewear. For illustration, POC's current material parameters are compared with DuPont's photopolymer, Polaroid's DMP-128, DCG and PVK (Table 3-1).

Table 3-1 Comparison of POC's Red-Sensitive Material with More Commonly Used Holographic Recording Materials

Material	Wavelength Range	Sensitivity mJ/cm^2	Maximum OD Attainable	Useful Thickness μm	Available Spectral Bandwidth nm	Moisture Protection Needed	Approximate Index Modulation Δn
POC's Red-Sensitive Material	600 nm to 2.7 μm	400	4-6	17-50	100-700	Yes	0.1-0.3
DCG	Visible to Near IR	200	5	5-25	10-150	Yes	0.1-0.2
DuPont Photopolymer	488-514 nm	30	3.4	7-20	10-25	No	<0.08
DMP-128	488-633 nm	30-60	3-4	7-15	10-100	Yes	0.06-0.08
PVK	488-532 nm	20-30	2.5	5-10	20-100	No	0.03-0.08
Silver Halide	488-633 nm	.001-0.01	0.7	2-7	30	No	<0.07

3.1.1 Red-Sensitive Materials

Dichromated gelatin (DCG) has been used as a holographic recording material, but with spectral sensitivity limited to wavelengths shorter than 514 nm. In order to increase DCG's spectral sensitivity, acid-fast violet B and methylene blue were used as a holographic recording material by Granbe [1] and Akagi [2] only to achieve diffraction efficiency of 50% at 633 nm. Kubota et al. [3] have also attempted recording holograms in red-sensitized DCG using methylene blue with ethlenediamine tetra-acetic acid (EDTA):Ammonia as a sensitivity enhancer. Recently, Changkakoti et al. [4] have studied the role of external electron donor in methylene blue-sensitized dichromated hologram. They have used EDTA, triethanloamine (TEA) and dimethylformamide as an electron donor, however, they obtained only about 71% diffraction efficiency. More recently, J. Blyth [5] has used tetramethyl guanidine as an electron donor to increase the sensitivity of DCG methylene blue recording material.

POC's latest efforts in developing red-sensitive holographic recording medium included:

(1) Selection of gelatin polymer graft system
(2) Choice of a sensitizer and a dye
(3) Choice of appropriate ratio of gelatin polymer graft: sensitizer: dye.

1. *Gelatin-Polymer Graft*

Although DCG exhibits ideal properties useful for volume phase holographic optical elements in the visible spectrum, there are significant potential drawbacks of DCG, and holographic optical elements based on it are easily affected by environmental changes such as temperature, pressure, humidity, etc. Realizing the importance of a holographic material that combines the advantages of a desirable holographic material, yet avoids the drawbacks of many of the gelatin materials, POC has developed a holographic recording material made from a gelatin-polymer graft. By modifying the molecular structure of gelatin by chemical or photo-chemical enriched grafting of polymerizable monomer, a novel material has been formulated which combines the high performance characteristics of DCG and photopolymers and avoids drawbacks of known holographic materials. The method of synthesizing gelatin polymer-graft involved attaching a polymerizable monomer to the backbone of gelatin. The choice of the monomer depended upon its compatibility with gelatin. Because of the gelatin-polymer interaction and integration at the molecular level, an increased number of cross-linking sites are generated. During exposure and processing, the crosslinks form a network of molecular chains which directly contribute to the refractive index modulation of the material. The enhanced crosslinks also harden the system, making it less sensitive to environmental changes, retaining the chemical composition intact under high temperature and pressure conditions.

2. *Choice of Sensitizer and Dye*

(a) DCG is known to have sensitivity to blue and green wavelengths. POC has developed in this program a recording material that is sensitive to the red part of the spectrum by choosing a methylene blue and ammonium dichromate as a dye and a sensitizer, respectively. However, as mentioned above, instead of gelatin, POC's new gelatin-polymer graft system was used.

(b) Another red-sensitive dye-sensitizer combination involved methylene blue/potassium chromate which were used along with POC's new gelatin polymer graft material and tetramethyl guanidine. Tetramethyl guanidine acts as an electron donor which enhances the sensitivity of the holographic coating. So far POC has used several electron donors including ethylenediamine tetra-acetic acid (EDTA), triethanol amine (TEA), N,N-dimethyl formamide (DMF), 1, 4 diazobicydo [2.2.2] Octane (DABCO), N,N,N,N-tetramethylene diamine (TMED) and 1,1,3,3-tetramethylguanidine (TMG). Among all the electron donors, TMG was found to be the most appropriate and effective for POC's red-sensitive recording material.

3. *Gelatin-Polymer, Sensitizer Dye Formulation*

As listed in Table 3-2, the coating formulation consisted of gelatin-polymer graft, sensitizer and a red-sensitive dye. The ingredient concentrations were adjusted per the requirement of peak wavelength in the near IR region as well as the optical setup used for recording.

Table 3-2 POC's Materials Used to Fabricate Broadband Near IR Filters

MATERIAL	SENSITIZER	DYE	ELECTRON DONOR	RESULTS
GPG	Potassium Chromate	Methylene Blue	TMG	High Diffraction Efficiency Excellent Thermal Stability
Gelatin	Potassium Chromate	Methylene Blue	TMG	High Diffraction Efficiency Moderate Stability
GPG	Ammonium Dichromate	Methylene Blue	TMG	High Diffraction Efficiency Moderate Stability
Gelatin	Ammonium Dichromate	—	—	High Diffraction Efficiency Moderate Stability

GPG = Gelatin Polymer Graft
TMG = Tetramethyl Guanidine

3.1.2 Experimental Preparation of the Red-Sensitive Coating

In a typical coating formulation, 30 to 75 grams of gelatin polymer graft were mixed in cold deionized water (300 to 500 ml) and the mixed mass was slowly heated to 60°C for about 2 hours to obtain a clear, homogeneous solution. To this solution, about 1-3 grams of potassium chromate were added after lowering the temperature of the water bath to 50°C. About half a gram of methylene blue was then added into the viscous solution followed by TMG solution until the pH was increased to about 9.5. In the event that the pH went up due to the addition of too much TMG, the pH was maintained between 9.1 and 9.5 by adding a few drops of acetic acid. The resulting solution was stirred until all the bubbles disappeared, and the froth, if any, was removed. The clear solution was then spin coated on a clean, dry glass plate (8" x 8") at a spinning rate of 33 to 78 rpm. The coated plates were stored in a laminar flow hood until dry. Generally, the age of the plate, for optimum exposure and results, was about 24 to 48 hours. The detailed process is summarized in Table 3-3.

Table 3-3 Procedure for Producing a Red-Sensitive Coating on Glass Substrates with a Spin Coating Technique

Step #	Directions	Comments	Room Light
1	Mix GPG polymer with cold water.	Stir with glass rod.	N/A
2	Heat slurry for 1-2 hr at 60 °C, stirring constantly.	Do not create bubbles while stirring	N/A
3	Add potassium chromate.	Bath temperature should be below 50 °C	Blue light
4	Add methylene blue powder.	Stir gently	Blue Light
5	Add TMG dropwise.	Maintain pH between 9.1-9.5	Blue Light
6	Heat viscous solution for 15 minutes and then filter it.	Temperature 45-50°C Use E-D #8 oz filter paper	Blue Light
7	Cast viscous solution on a clean glass plate	Spin the plate at 33-78 rpm	Blue Light
8	Keep coated plate at room temperature for 24 hours	Keep plate horizontal until it is dry.	Blue Light

3.1.3 Exposure and Recording Conditions for IR Broadband Filters

The exposure setup used is illustrated in Figure 3-2. As the laser beam (633 nm) incident on the polymeric emulsion is reflected from the front surface of the mirror, interference fringes are found in the emulsion. The dark and bright fringes of the pattern create a hardness differential, thereby producing layers of high and low refractive index. The index differential process is further enhanced by wet processing (see Table 3-4), resulting in structures that reflect a broadband of wavelengths in a manner similar to a multilayer dielectric interference filter. During the Phase I contract period, a number of broadband IR filters were fabricated by this process. A few of the filters' spectral curves are illustrated in Figures 3-3 and 3-4. These filters have optical density greater than four, while their bandwidths exceed 200 to 400 nm. Moreover, photopic/scotopic transmission is about 65% to 75%. The peak wavelength varies from 625 nm to 1 μm and above.

In the present investigation, a peak wavelength for near IR broadband filters for up to 1.5 μm has been measured, however, longer peak wavelengths can also be achieved by (i) chemical/material

swelling or (ii) by increasing the angle of incidence, with a limit set by the critical angle of the air-substrate interface. By eliminating the interfacing problem with the use of index-matching liquid, the critical angle limit can be increased. See Figure 3-5(a) and (b) for an illustration.

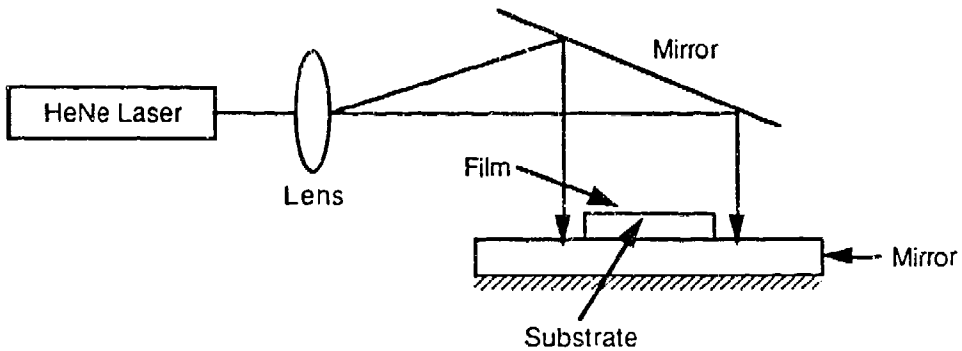

Figure 3-2 Illustration of an Optical Setup for the Fabrication of Near IR Broadband Filters Using Potassium Chromate as a Sensitizer.

The large angle recording design as shown in Figure 3-5(a) and (b) helps to achieve high non-uniform spacing, $\Delta\Lambda$, and high index modulation. Because θ_m is large, a laser beam has to travel a longer path (several times the emulsion thickness) in the recording medium. The absorption of light by the medium is increased, thus creating a large differential of hardness in the thickness of the medium. This results in large $\Delta\Lambda$. The angle of recording, θ_m, is larger than the critical angle θ_c of the medium (which is 42° in this particular case). Thus, the back reflection is a total internal reflection (TIR), 100%. Therefore, the two recording beams (incident and reflected beams) have an almost 1:1 intensity ratio, resulting in very high contrast fringes. Therefore, maximum index modulation, Δn, is achieved for the particular recording and processing conditions.

The spectral plots of typical broadband filters fabricated using this experimental setup are illustrated in Figures 3-6 and 3-7.

Table 3-4 Procedure for Fabrication of a Broadband IR Filter

Step #	Directions	Comments	Lighting Conditions
1	Expose coated plate to HeNe laser (633 nm)	Normal incidence or prism/cube aided exposure	Blue light
2	Soak the plate in fixer for 20 sec-1 min.	With agitation	Blue light
3	Place the plate in room temperature water for 2-4 min.	No agitation needed	Blue light
4	Soak in 25% isopropyl alcohol for 1-3 min.	With agitation	Blue light
5	Soak in 50% isopropyl alcohol for 1-3 min.	With constant agitation	Blue light
6	Soak in 75% isopropyl alcohol for 2-3 min.	With constant agitation	Blue light
7	Soak in 100% isopropyl alcohol for 2 min.	With constant agitation	Blue light
8	Soak in 100% isopropyl alcohol at 65 $^{\circ}$C for 30 sec-1 min.	With constant agitation	Blue light
9	Dry with blow dryer.	With constant movement	Blue light

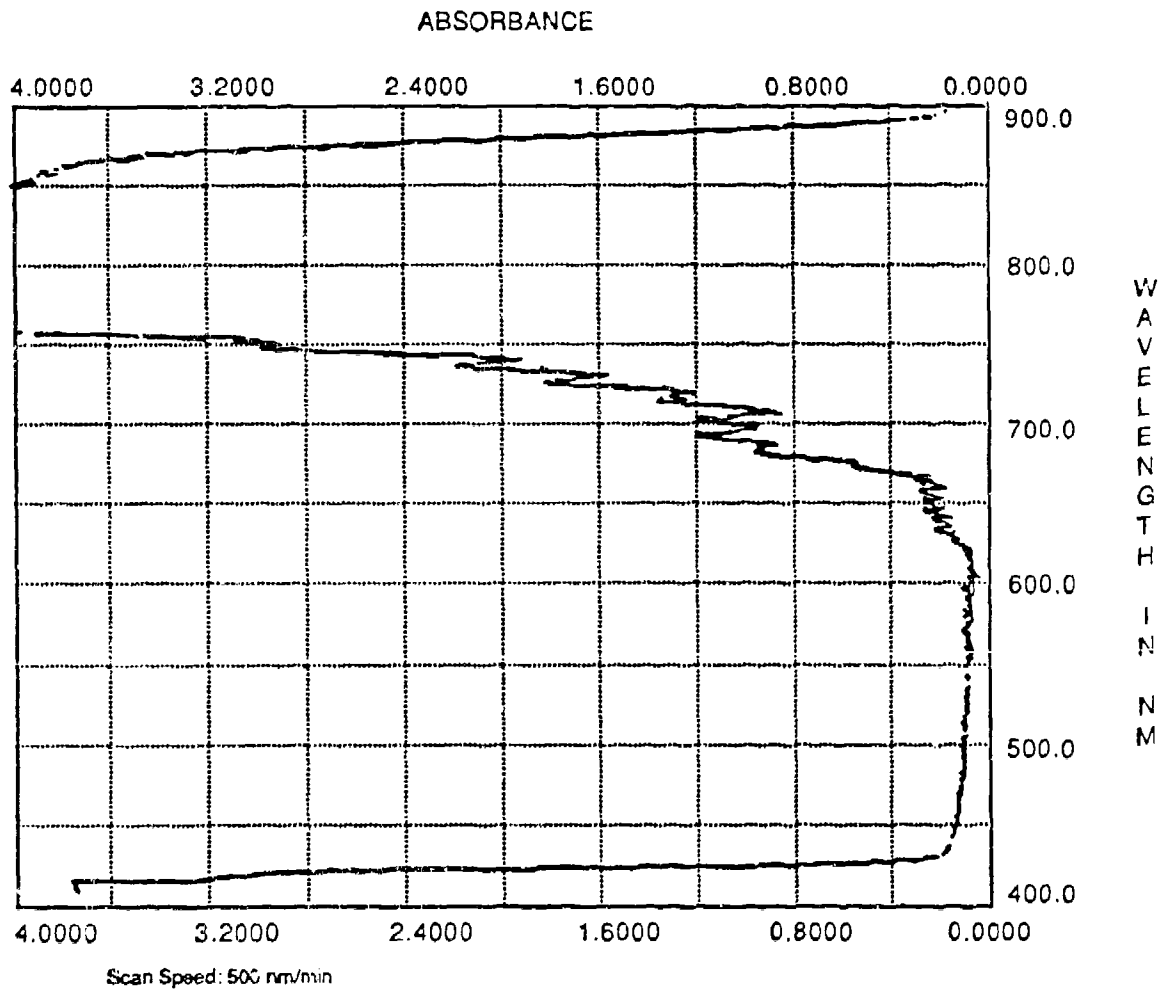

Figure 3-3 Illustration of a recently fabricated POC red-sensitized filter of optical density greater than 4 and a bandwidth of about 70 nm.

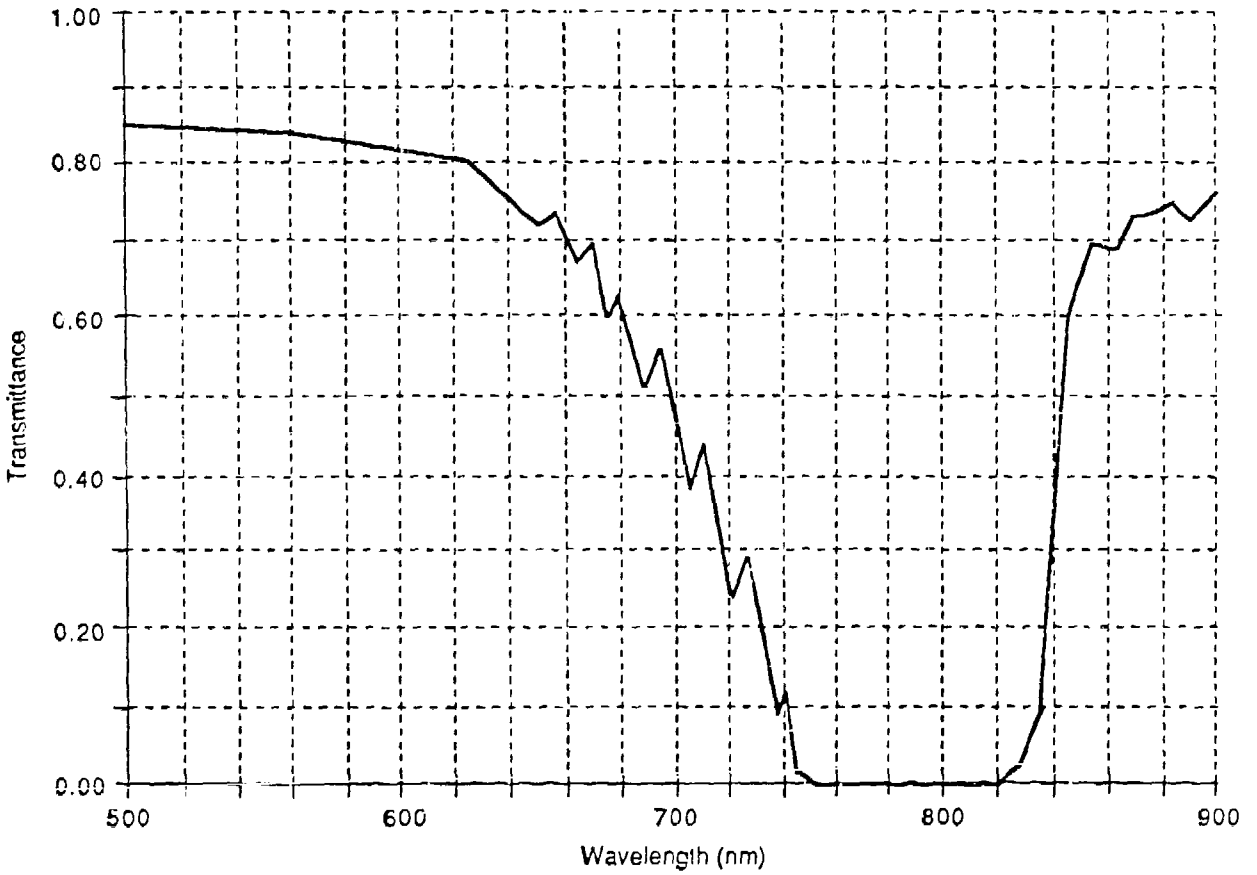

Figure 3-4 Illustration of a POC broadband filter fabricated in red-sensitive material with optical density greater than 4 and a bandwidth greater than 200 nm.

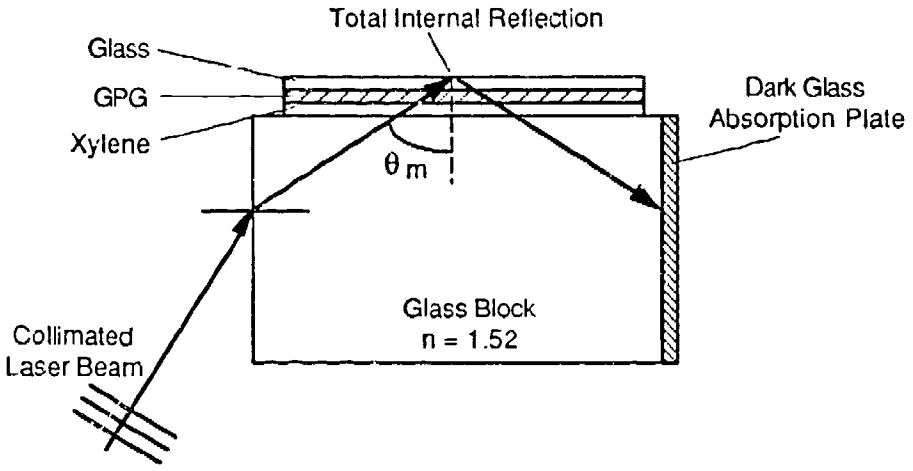

Figure 3-5(a) Holographic recording setup used to fabricate broadband IR filters. Using this setup, eye protection for longer wavelengths (of 2 μm) can be accomplished.

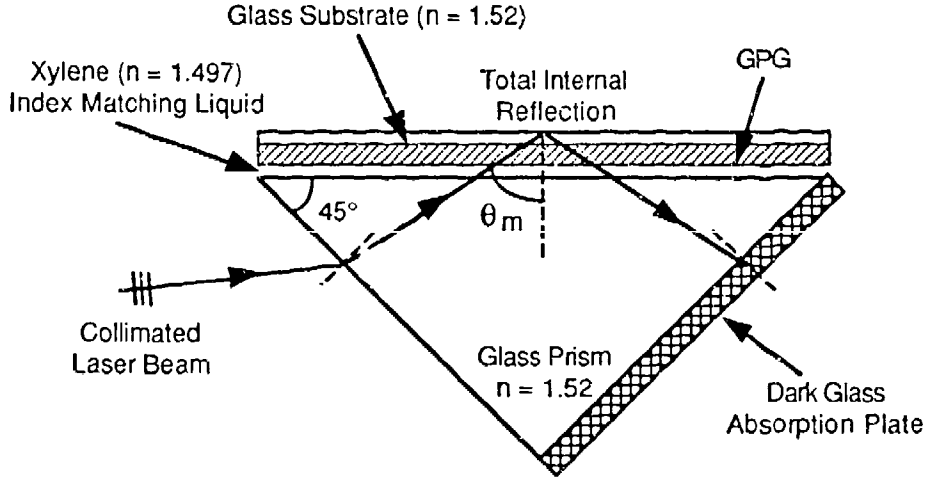

Figure 3-5(b) Holographic exposure setup used to fabricate long-wavelength laser eye protection filters with broad bandwidth.

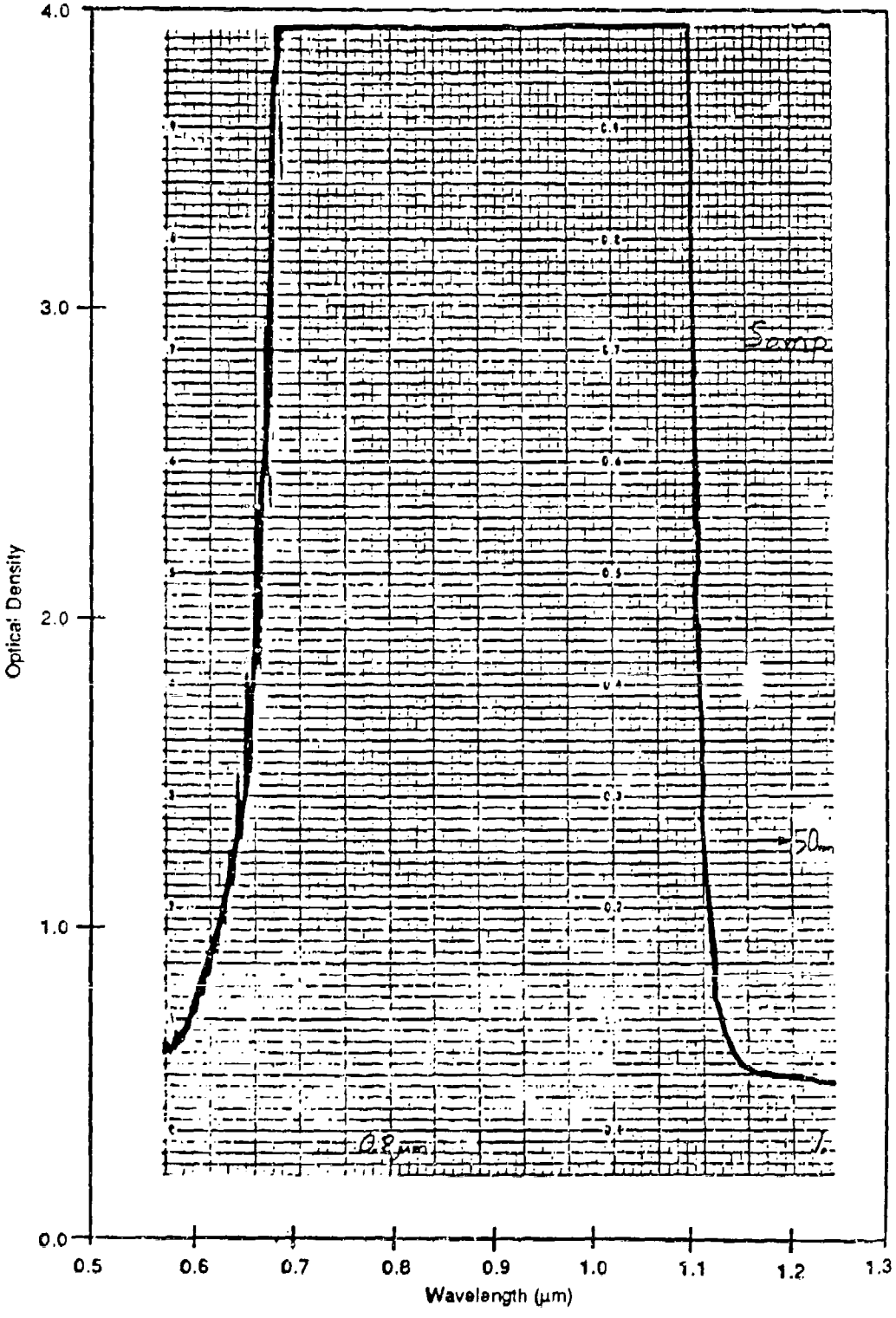

Figure 3-6 Illustration of a broadband protection filter where the cut-on wavelength is 650 nm and the cut-off wavelength is 1140 nm.

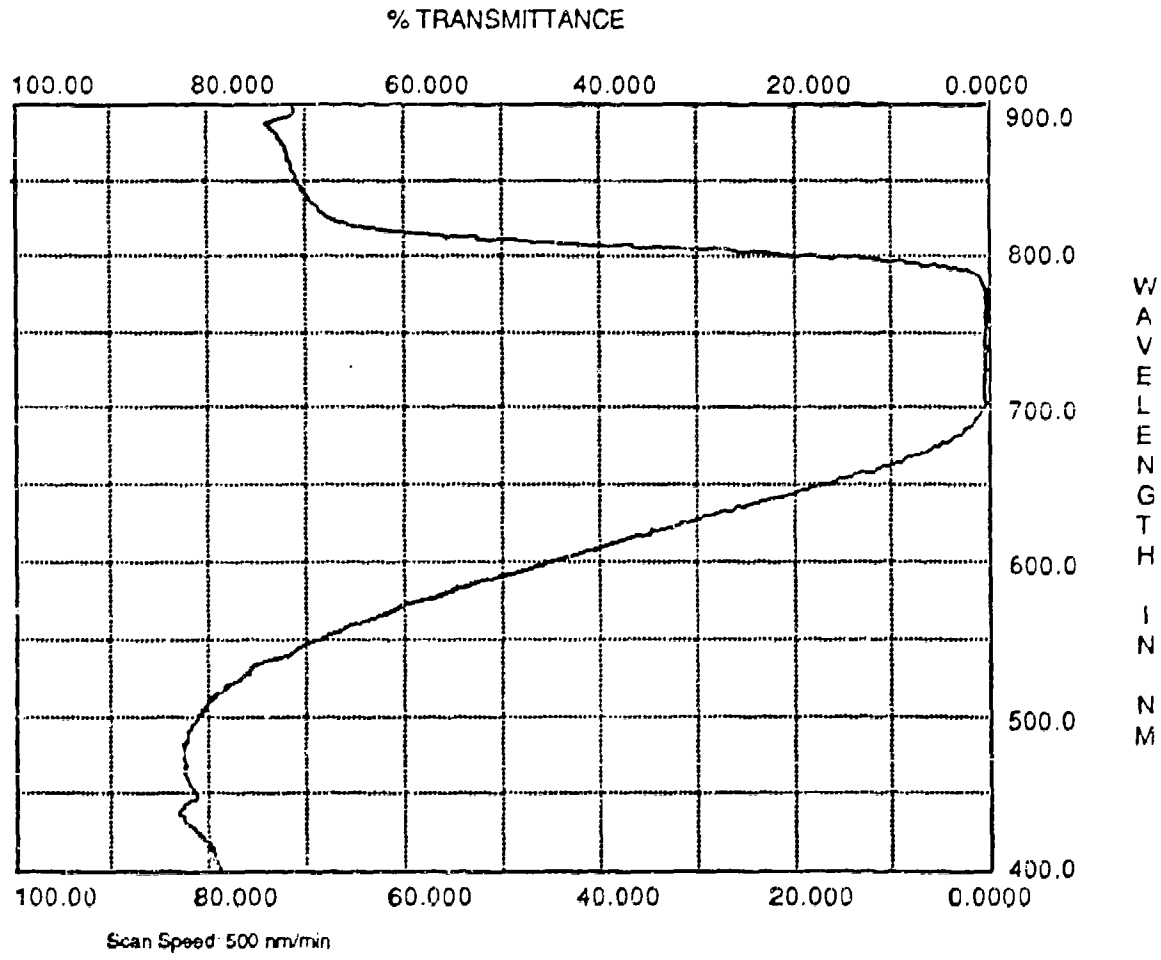

Figure 3-7 %-transmission vs. λ curve for BLEP filters based on red-sensitive material.

3.2 Angular/Bandwidth Characteristics BLEP Filters

In the material that follows, we will discuss only those holographic characteristics that are useful for meeting the technical goals of the Phase II program and which are worthy of review.

Conventionally, the protection wavelength, λ_p, is simultaneously the central peak wavelength, λ_o, for normal incidence, i.e.,

$$\lambda_o = \lambda_p \qquad \text{for } \theta' = 0 \tag{3-1}$$

where θ' is the angle of incidence in the holographic medium (see Figure 3-8(a)). It will be shown that the profile of the hologram's spectral characteristics changes only slightly as the angle of incidence is increased (see Figure 3-8(b)), while the hologram's central peak wavelength shifts to the blue, according to the following relation

$$\lambda_o' = \lambda_o \cos\theta' \tag{3-2}$$

where the measured angle of incidence (in air), θ, and the angle θ', are related through Snell's law

$$\sin\theta = n \sin\theta' \tag{3-3}$$

In order to verify Eq. (3-2), let us examine the fundamental results of Kogelnik's theory (H. Kogelnik, Bell Syst. Tech. J., 48, 249 (1969)), as it relates to holographic filters. In the case of Lippmann holograms (fringe planes parallel to the surface), Kogelnik's formula for diffraction efficiency has the form

$$\eta = \left[1 + \frac{\left(1-\xi^2/\nu^2\right)}{\sinh^2\sqrt{\left(\nu^2-\xi^2\right)}}\right]^{-1} \tag{3-4}$$

where sinh is the hyperbolic sine and ξ and ν are two auxiliary parameters that have the following forms for Lippmann holograms

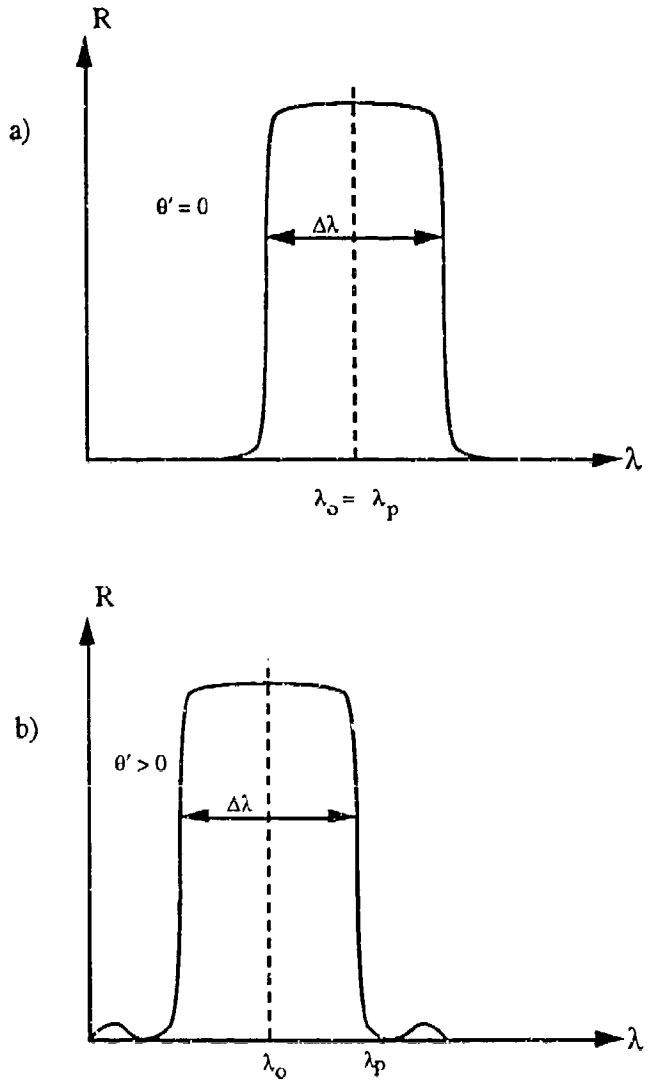

Figure 3-8 Holographic bandwidth blue-shift (a) for normal incidence and (b) off-normal angles of incidence for conventionally-recorded holograms.

$$\xi = 2\pi\bar{n}T\left(\frac{\cos\theta'}{\lambda} - \frac{1}{\lambda_B}\right) \tag{3-5}$$

$$\nu = \frac{\pi\Delta n T}{\lambda\cos\theta'} \tag{3-6}$$

where $\bar{n}$ is the average refractive index, Δn is the refractive index modulation, T is the hologram thickness, λ_B is the Bragg wavelength (in vacuum), and θ' is the angle of incidence (in this

holographic medium) that is related to the angle of incidence in air, θ, by Snell's relation (3-3). The parameter ξ is called the off-Bragg parameter because it describes how far we are from the Bragg condition (where ξ = 0).

We can see that the Bragg wavelength λ_B is close to the peak wavelength only for normal incidence. In general, the condition ξ = 0 is equivalent to

$$\lambda'_0=\lambda_0 \cos\theta'=\lambda_0\sqrt{1-\sin^2\theta/\bar{n}^2} \tag{3-7}$$

Only for θ' = 0 is $\lambda'_0 = \lambda_0$. For larger angles of incidence , the Bragg wavelength shifts to shorter wavelengths. This effect is easy to observe experimentally.

The second Kogelnik parameter, ν, is called the coupling constant because it characterizes how strongly a diffractive wave is "coupled" with the incident wave. In other words, within the hologram bandwidth, the diffraction efficiency is a monotonically-increasing function of ν (for fixed ξ); that is, the ν parameter characterizes the diffraction power of the hologram. In the on-Bragg case (ξ = 0), the basic Eq. (3-4) reduces to the following

$$\eta = \tanh^2\nu \tag{3-8}$$

where tanh is the hyperbolic tangent.

Comparing Eqs. (3-2) and (3-7) and zeroing the off-Bragg parameter in Eq. (3-5), we can see that the peak wavelength indeed shifts to blue for slanted angles of incidence, while, according to Eq. (3-4), the hologram spectral profile changes only slightly.

For the conventional recording case, Eq. (3-1) is satisfied; thus, Eq. (3-2) can be rewritten

$$\lambda'_o = \lambda_p \cos\theta' \tag{3-9}$$

and

$$\lambda'_0=\lambda_p-\frac{\Delta\lambda}{2} \tag{3-10}$$

where $\Delta\lambda$ is the hologram spectral bandwidth as illustrated in Figure 3-8. Using Eqs. (3-9) and (3-10), we obtain

$$\cos\theta' = 1 - \frac{\Delta\lambda}{2\lambda_p} \tag{3-11}$$

or,

$$\frac{\Delta\lambda}{2\lambda_p} = 1 - \cos\theta' \tag{3-12}$$

Using Eqs. (3-12) and (3-7) for n = 1.55 (DCG) and a wavelength of λ_p = 694 nm, we obtain a fundamental relation between the angular protection and the hologram bandwidth presented in Table 3-5. We can see that for ± 30° angular acceptance in air (i.e., θ = 30°), the bandwidth is quite broad, namely 70 nm.

Table 3-5 (a) Relation between the angular protection and the required bandwidth using the red-shift tuning method for 694 nm. (b) Bandwidth versus angular protection for the conventional method of wavelength protection for n = 1.55 and a protected wavelength of 694 nm.

ANGULAR PROTECTION (θ in deg)	10	20	30	40	50	60
$\Delta\lambda$ (nm) at λ_p = 694 nm	4.1	14	35	65	96	128

(a)

θ	10°	20°	30°	40°	50°	60°
$\Delta\lambda$ (nm)	8	34	70	124	180	236

(b)

However, it will be shown in what follows that the bandwidths can be significantly reduced by using a red-shift-tuning-based approach. Thus, one can anticipate obtaining full angular protection for the visor configuration while still maintaining high scotopic/photopic efficiencies. This will be demonstrated later.

The red-shift tuning method is illustrated in Figure 3-9. It can be seen that even for the normal incidence case the peak protected wavelength does not coincide with the central peak wavelength, but rather that it is located at the extreme blue side of the hologram spectral characteristic according to

$$\lambda_o = \lambda_p + \frac{\Delta\lambda}{2} \tag{3-13}$$

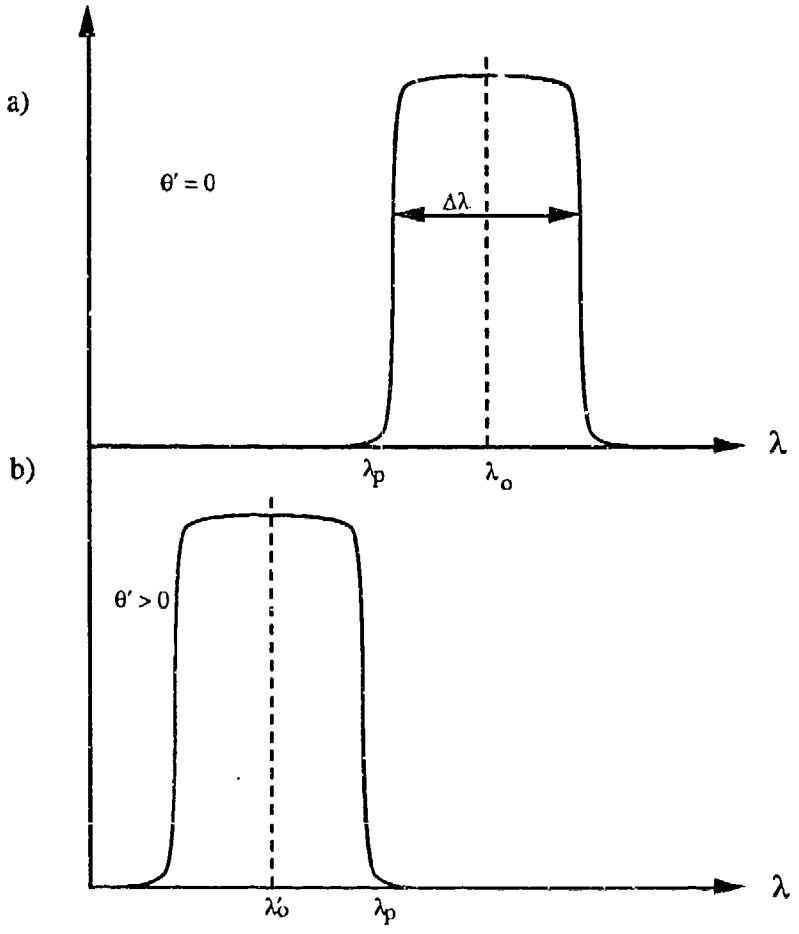

Figure 3-9 Illustration of a Slanted-Angle Blue Shift Using the Red-Shift Tuning Method Including Normal Incidence Case (a) and Slanted Angle Case (b).

Therefore, the slanted-incidence blue shift (see Figure 3-9(b)) can be approximately twice as effective as that of the conventional recording (see Figure 3-8(b)). Accordingly

$$\lambda_o' = \lambda_p - \frac{\Delta\lambda}{2} \tag{3-14}$$

Thus, instead of Eq. (3-11), we obtain

$$\cos\theta' = \frac{\lambda_o'}{\lambda_o} \tag{3-15}$$

or

$$\cos\theta' = \frac{\lambda_p - \Delta\lambda/2}{\lambda_p + \Delta\lambda/2} \tag{3-16}$$

and, finally, using Eqs. (3-13) to (3-16) we obtain

$$\frac{\Delta\lambda}{2\lambda_p} = \frac{1-\cos\theta'}{1+\cos\theta'} \tag{3-17}$$

This is the fundamental equation representing the red-shift tuning method. Comparing Eq. (3-17) with the conventional bandwidth recording, Eq. (3-12), we recognize that the additional factor in the denominator is approximately equal to 2 for small angles of incidence. Therefore, for the same angular protection, the red-shift required bandwidth is approximately two times narrower than that for the conventional case.

The new relation between the angular protection and the required bandwidth has been demonstrated (for n = 1.55) for 694 nm in Table 3-5(a). When compared with Table 3-5(b) we can see that, indeed, the required bandwidths are approximately two times smaller. For example, for $\theta = 30°$, we have the red-shift tuning required bandwidth of 35 nm while the conventional bandwidth is twice as large, namely 70 nm.

As shown above, the intrinsic characteristics of an interference filter are angle dependent. However, by being able to accurately position the left edge of the interference filter so that it barely covers the threat wavelength, one can either increase the angular protection by 50% or decrease the bandwidth, $\Delta\lambda$, by a factor of two to obtain a given angular protection. In performing work for major programs sponsored by DARPA and SDI over the past year, POC has been able to develop repeatable volume holographic filters in which the bandwidth characteristics can be adjusted to within 2 nm.

3.3 Geometry-Dependent Notch Filters

Many authors [6,7,8] have noted that for recording holographic notch filters on curved substrates (either singly or doubly curved), a geometry-dependent wavefront is needed to optimize the resulting performance of the filter and to minimize optical aberrations.

In order to prevent laser rays from entering the pupil of an eye situated behind a flat substrate, an angular protection of 20° (35 nm bandwidth) suffices for that portion of the substrate directly in front of the eye. However, as one moves outward from this position, even the red-shift tuning method previously discussed can supply only a 30° angular coverage when, in actuality, greater than 40° is required.

The single most important difference between holographic technology and dielectric stack multilayer coatings is that the reflective layers for holographic mirrors do not have to follow the same geometry as the substrate upon which they are placed. On the other hand, dielectric stacks must have the same geometry as the substrate upon which they are deposited. We will now show that this single attribute of holographic technology is absolutely crucial for meeting Army requirements for full angular protection of the eye.

The optical characteristics of holographic mirrors do not need to be the same as the geometry of their substrate. Plane, spheric, or aspheric holographic mirrors can be produced on a plane or any other substrate. In recording the hologram, all that is required is that the wavefronts reaching the substrate (on which the recording material is placed) converge or diverge from spatial points coincident with the foci of the corresponding conic section. These geometric foci will become the foci of the optical holographic mirror [6].

Consider the particular case of a holographic notch filter used on a spectacle lens. If the holographic notch filter is recorded from a spherical wavefront (pinhole) with its center of curvature coincident with the center of rotation of the eye, then all of the rays incident to the center of the eye will be normal to the holographic mirror and will have a constant 0° angle of incidence. The size of the pupil of the eye and the rotation of the eye make it necessary to allow for small angles of incidence (Figure 3-10) that can be accepted for this finite geometry. Still, these small angles, ±9° at the center and approximately ±16° at the edges, will not significantly reduce the photopic or scotopic transmission.

Approaches similar to the spectacle-eye geometry can be applied to the Army visor. A holographic elliptical mirror with each of its foci at the center of an eye (Figure 3-11) will achieve total field coverage for the Army visor. Analogous to the spectacle case above, the size of the effective pupil will require small angles of incidence tolerances (12.3° to give total protection for the Army visor geometry).

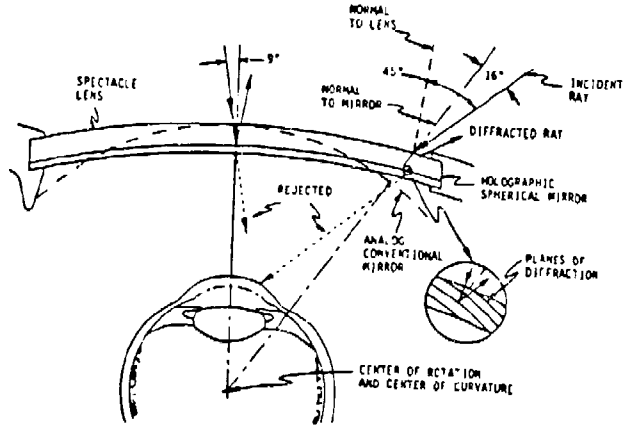

Figure 3-10 Spectacle-Eye Geometry With a Holographic Spherical Notch Filter Providing Wide Angular Protection (J. Margarinos and D. Coleman, Applied Optics, Vol. 26, No. 13, p. 2576, July 1987).

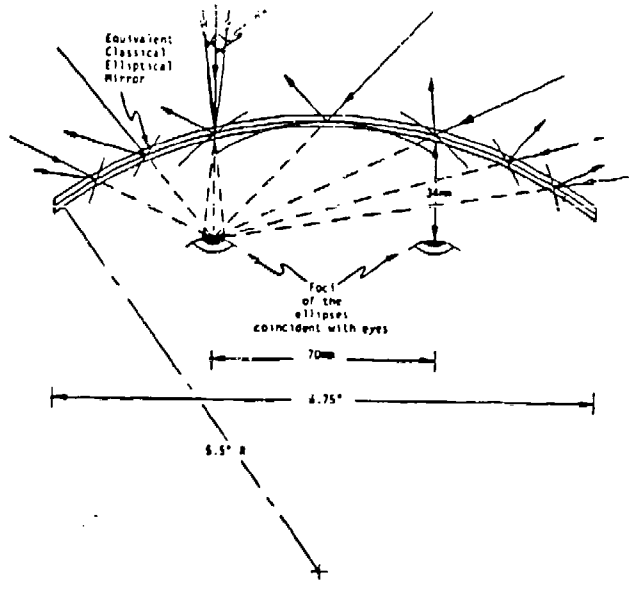

Figure 3-11 Goggle-eye geometry with a holographic elliptical notch filter providing wide angular protection (J. Margarinos and D. Coleman, Applied Optics, Vol. 26, No. 13, p. 2576, July 1987).

3.4 Near IR Bandwidth

A broadband near IR rejection filter which cuts on at 690 nm, has a bandwidth of 450 nm and cuts off around 1140 nm was modeled by POC. The results showed a photopic efficiency of 84.68% and a scotopic efficiency of 84.99%. This assumes an out-of-band transmission in the visible spectrum of 85% (a number consistently achieved experimentally). We have projected a photopic/scotopic efficiency of 75% because the filters do not cut on instantaneously (i.e., there is some slope to them, but it is very steep).

The characteristics of POC's broadband near IR filters are shown in Figures 3-12(a) and (b), and 3-13. Their present OD is typically greater than three over a large portion of the IR spectrum.

The factors involved in achieving a very broad bandwidth in the IR region include:

(i) thickness
(ii) optimum sensitizer, dye, and electron donor concentration
(iii) optimum exposure
(iv) recording angle
(v) processing

These parameters are more or less interconnected, therefore, optimal thickness (50-100 μm), dye-sensitizer concentration (0.1-1%), exposure of 200 to 400 mJ/cm^2 and optimal processing conditions are required to achieve broadband, high optical density, and high photopic/scotopic efficiency filters. Because the filter operates in the IR region and the material is transparent in the visible range, photopic/scotopic efficiencies are naturally high. An approximate angular formula for such a non-uniform Lippmann holographic filter is given by Jannson et al. [9] where reference is made to Figure 3-14.

$$\frac{\Delta\lambda'}{\bar{\lambda}_B} = \frac{\Delta\lambda}{\lambda_B} + \frac{\Delta\Lambda}{\bar{\Lambda}} \qquad (3\text{–}18)$$

where

$\Delta\lambda'$ = bandwidth of the non-uniform hologram
λ_B = Bragg wavelength
$\Delta\lambda$ = bandwidth for the fully-uniform case
$\Delta\Lambda$ = grating constant range
$\bar{\Lambda}$ = average Bragg grating constant

The Bragg bandwidth for Kogelnik's fully uniform case (high efficiency) is given by [10]

$$\frac{\Delta\lambda}{\lambda} = \frac{1}{\cos 2\phi} \frac{\Delta n}{n} \tag{3-19}$$

For normal incidence ($\phi = 0$), Eq.(3-18) becomes

$$\frac{\Delta\lambda'}{\lambda} = \frac{\Delta n}{n} + \frac{\Delta\Lambda}{\Lambda} \tag{3-20}$$

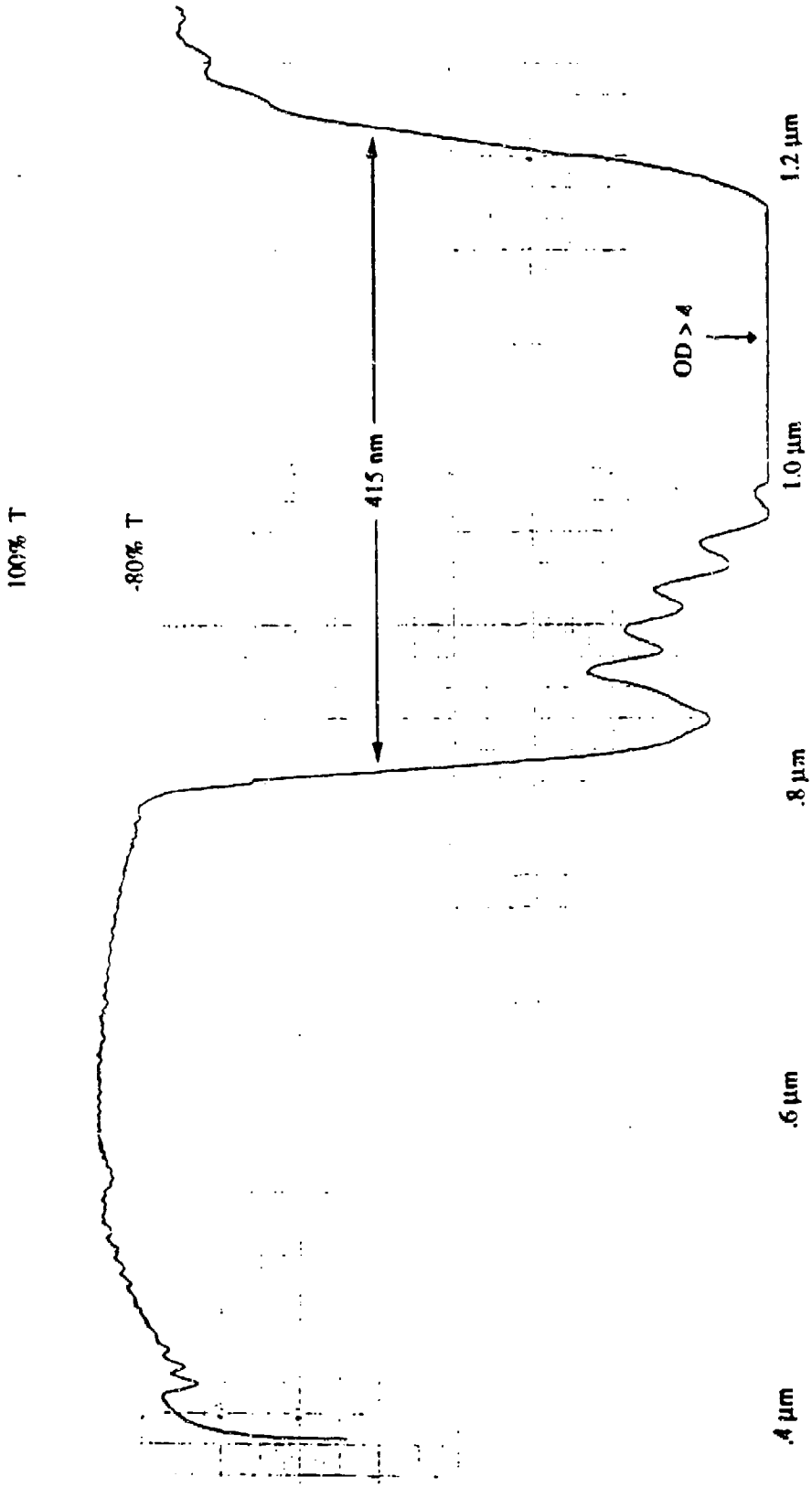

Figure 3-12(a) Experimental spectrophotometer plot of POC's existing solar control filter.

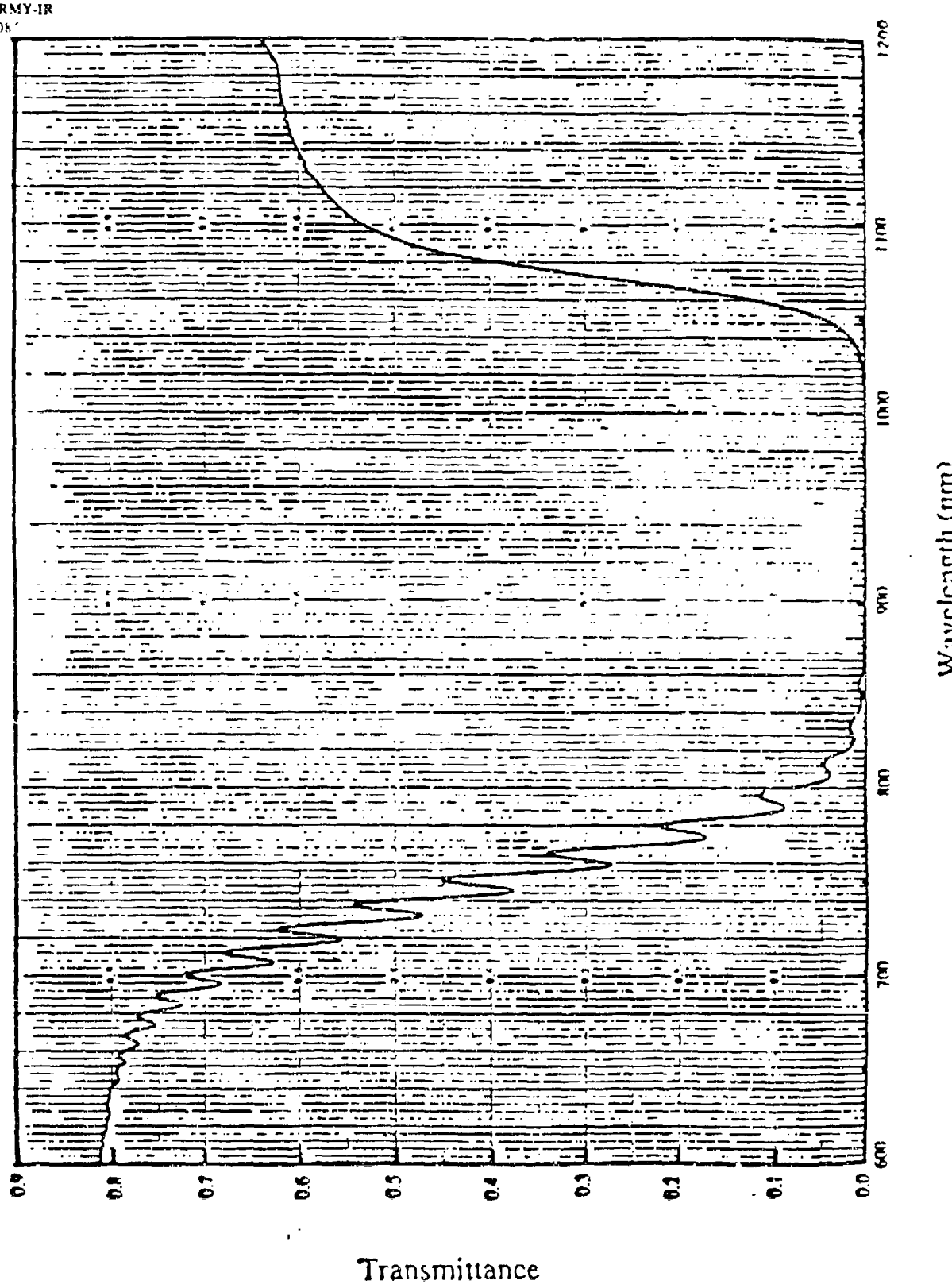

Figure 3-12(b) Illustration of POC's broadband transmission plot. The filter was recently fabricated in POC's Optics Laboratory.

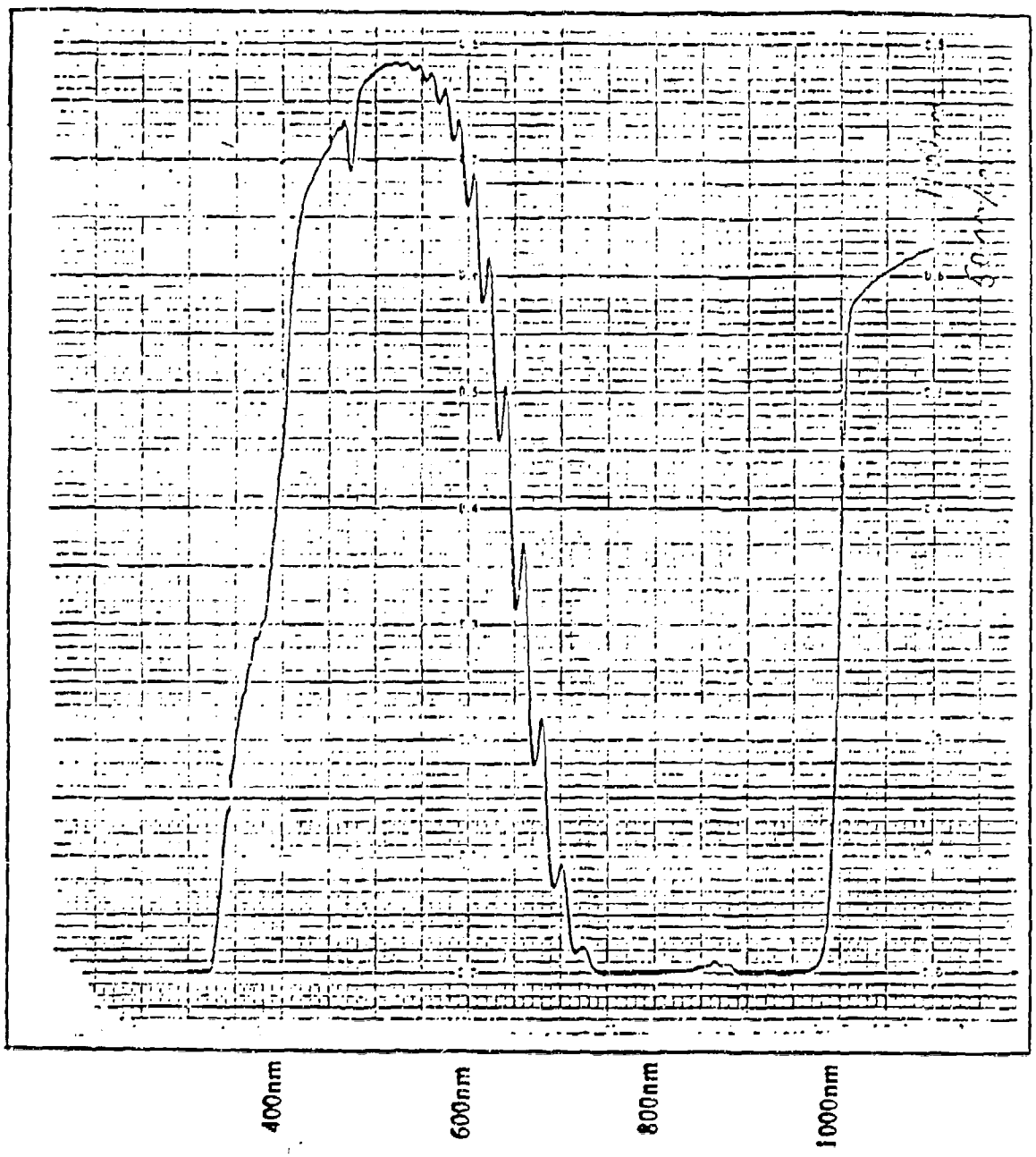

Figure 3-13 POC's new holographic filter for protecting against Nd:YAG fundamental wavelength 1.06 μm: a broadband application.

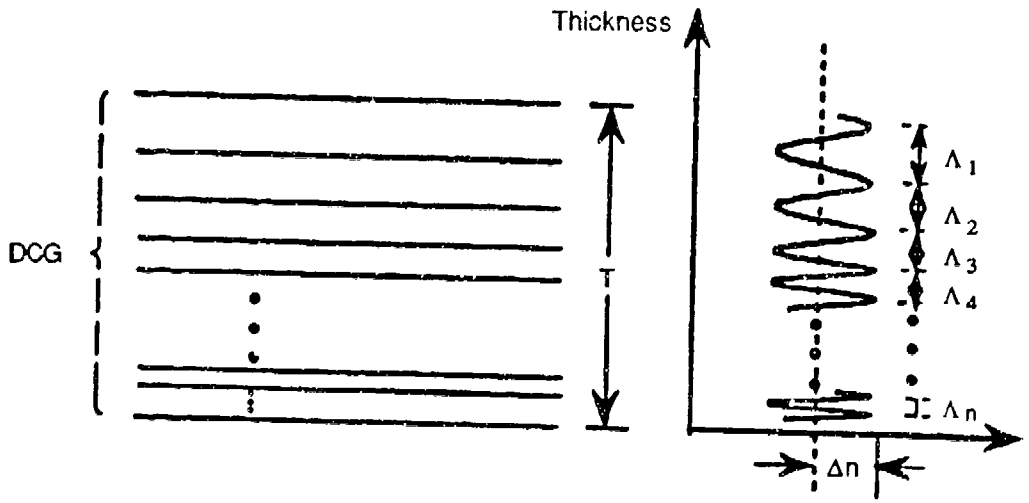

Figure 3-14 Non-uniform Bragg planes in DCG Lippmann holograms.

3.4 Chemistry of Red-Light Sensitive (RLS) Holographic Recording Material

The chemical mechanism of the crosslinking reaction that takes place inside the coating in red-sensitive material is very similar to that of a DCG holographic coating. Because whether ammonium dichromate [$(NH_4)_2Cr_2O_7$] or potassium chromate (K_2CrO_4) is used as sensitizer, the valency of chromium remains 6 which is reduced to Cr^{+3} during exposure and processing. Cr^{+3} ions form coordination complex with $CO\overline{O}$, hydroxy and amino groups of DPX-1 and IRT-6 polymers. These coordination complexes develop crosslinks between chains, thus enhancing the rigidity of the gelatin or gelatin graft polymer and making it less soluble in water.

The polar groups that are present in the gelatin or graft polymer may be linked to polar-uncharged side chains by a hydrogen bond or to polar-charged sites by a bipolar interaction thereby establishing chemical bridges between amino acids, peptides or gelatin polymer molecules as illustrated in Figure 3-15. During processing, the crosslinking process is strengthened creating a hardness differential between highly-crosslinked and lightly-crosslinked regions. This hardness differential that creates the density differential is further enhanced by the chemical nature and size of the chemical groups of DPX-1 and IRT-6 polymeric materials. This hardness differential is responsible for the high refractive index modulation necessary for the formation of high-efficiency broadband IR filters. The physical phenomenon of refractive index modulation can be confirmed by taking cross-sections of BLEP filters, metallizing them with extremely thin silver or gold layers

and then observing them with a scanning electron microscope. This is shown in Figure 3-16 where the theoretically calculated grating spacing, $\Delta\Lambda$ = 167 nm, corresponds to the experimentally observed $\Delta\Lambda$ (Bragg spacing).

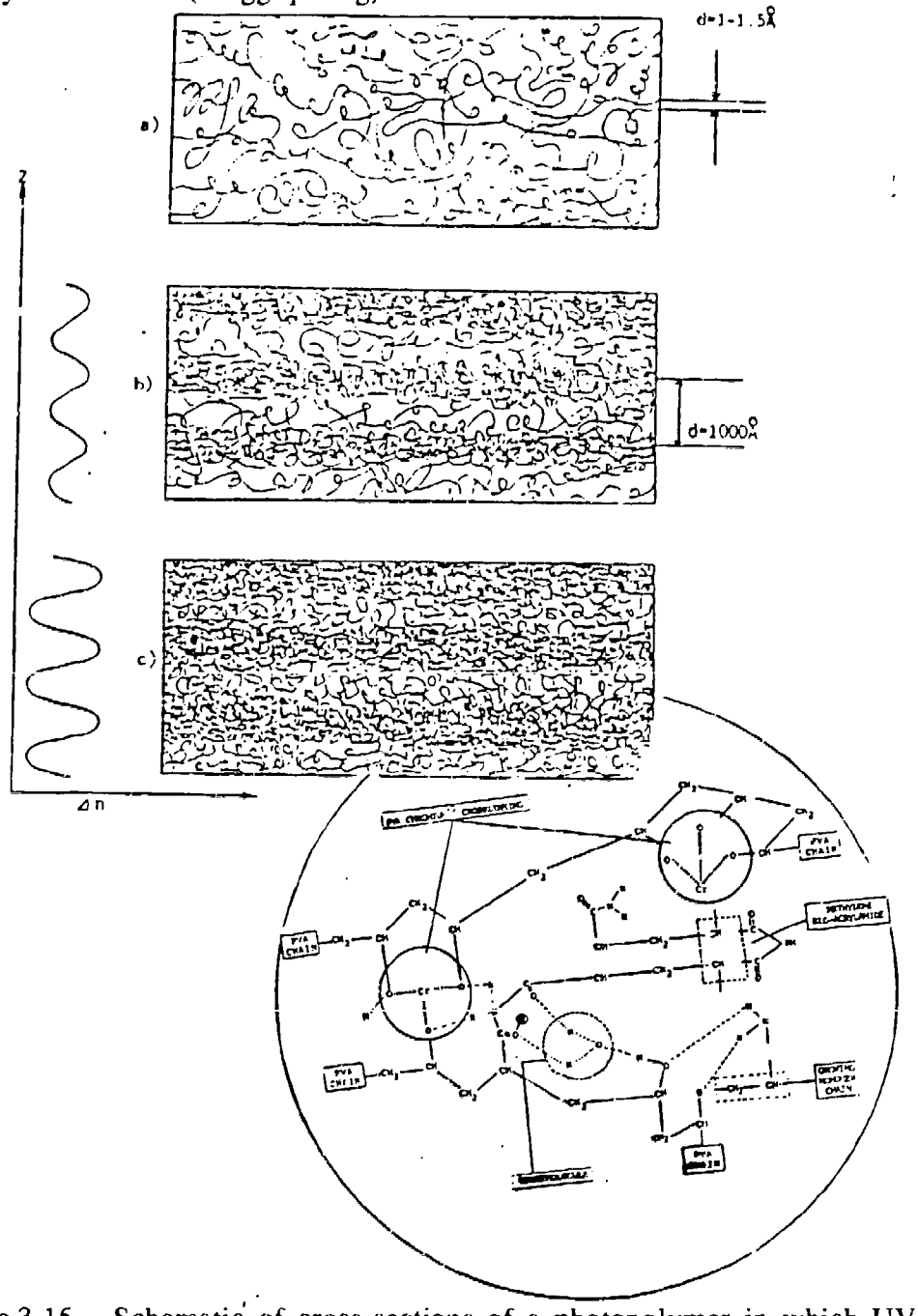

Figure 3-15 Schematic of cross-sections of a photopolymer in which UV volume holographic gratings are being created by: (a) exposure to light, (b) dark reaction/partial fixing, and (c) fixing and processing. The final material density modulation (resulting in refractive index modulation) is caused by grafts and/or highly crosslinked macromolecular webs that reside in separate Bragg planes.

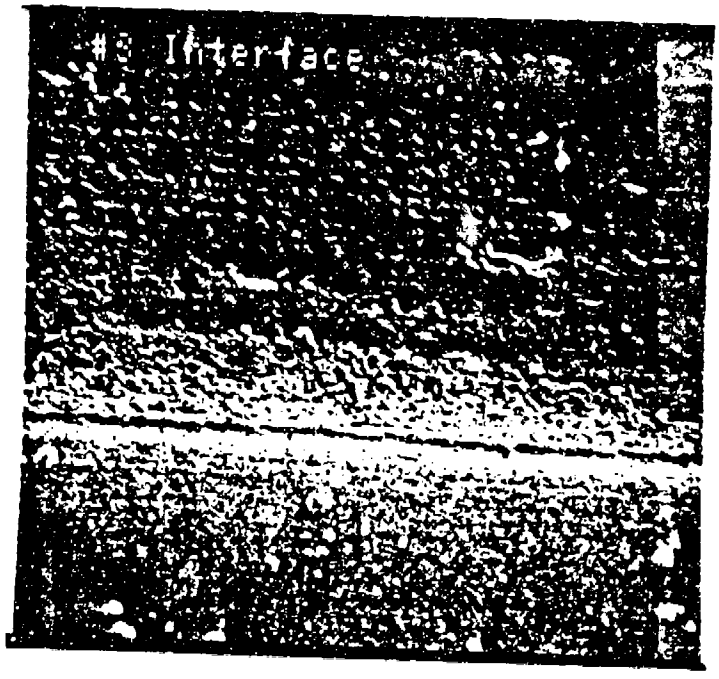

Figure 3-16 Scanning Electron Micrographs of Cross-Section of Holographic Filters.

3.5 Lightweight Inexpensive Substrate Evaluation

A flat glass plate would be an ideal substrate for POC's BLEP filters but it is too heavy, expensive, and does not withstand the ballistic requirements. Therefore, POC investigated a number of plastic substrates that are transparent in the visible to near IR spectrum including polycarbonate (PC), polymethyl methacrylate (PMMA), polystyrene (PS), polyvinyl-chloride (PVC), Aclar and styrene-acrylic copolymers (NAS) and TPX. All of these plastics have over 90% visible light transmission which make them comparable to glass. PMMA, PC, Aclar, and TPX are superior to glass in terms of ultraviolet light transmission. In addition, most of these plastic substrates are over 90% transparent up to 1120 nm as illustrated in Figure 3-17. The physical properties of these optical plastics are listed in Table 3-6. The data from Table 3-6 indicate that PC, Aclar and TPX are the best substrate materials because they have excellent transparency, impact strength, and low moisture absorptivity.

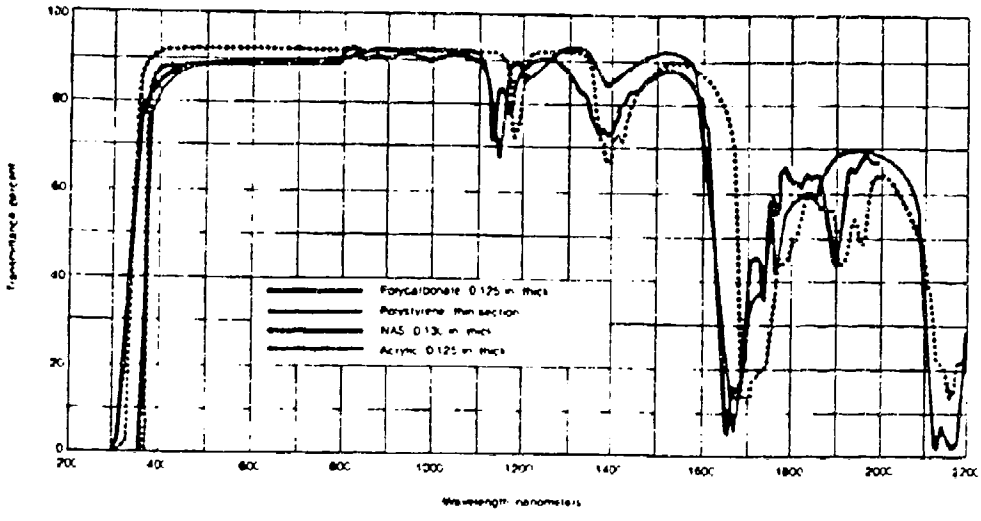

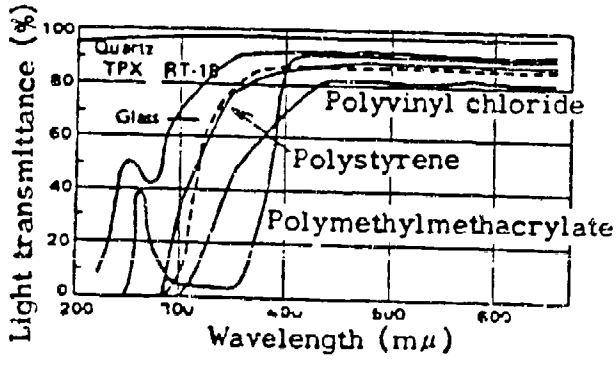

Figure 3-17 Transmission Characteristics of Principal Optical Plastics.

Table 3-6 Physical Properties of Transparent Plastic Substrates Suitable for BLEP Filters

Properties	PMMA	PC	Aclar	TPX	P5	PVC	NAS
Refractive Index	1.491	1.586	1.43	1.46	1.59		
Luminous Transmission	92%	92%	92%	92%	92%	92%	90
Maximum Continuous Temperature °F	175	240	280	>200	175		175
Water Absorption (Immersed 24 hr at 73 °F)	0.3%	0.15%	0.03	0.10	0.2		
Impact Strength (ft-lb/in)	0.5	15	>100	40	0.35		
Dielectric Strength (v/mil)	500	400	>500	>500	500		
Coefficient of Thermal Expansion (Linear)	3.6	3.8	3.3-3.6	3.4	3.5		

3.6 Coating Fabrication Technology

Unlike dielectric multilayer technology, POC's holographic recording material does not require the use of expensive coating equipment. In fact, a simple overhead spinner is sufficient to fabricate the smooth, continuous and uniform film needed for the holographic BLEP filters. Other coating methods found to be successful include spin, web, dip, doctor's blade, and casting. Details of these methods are summarized in Table 3-7. In the spinning method, the thickness of the coating depends on the solution temperature, the viscosity of the solution, and the spin rate whereas in the other methods (i.e., web, dip, doctor's blade, casting) the thickness depends on the movement of the blade or the thickness of the spacer. The methods described in Table 3-7 can be used for many of the substrates listed in Table 3-6.

Table 3-7 POC's Coating Methods That Use Glass or Plastic Substrates

Method	Size Range	Coating Thickness Range
Spin Coating	<1 m^2	1 - 100 μm
Web Coating	15 mm^2 to 1.5 m^2	2 - 40 μm
Casting	0.5 m^2	5- 500 μm
Doctor's Blade	1 m^2	1 - 100 μm
Dip Coating	0.5 m^2	1 - 50 μm

3.7 Environmental Studies of BLEP Filters

Gelatin, DCG and gelatin-based graft polymers RTX-2 and IRT-6 are soluble in water, therefore, the holographic elements made from these materials need to be protected against humidity. Otherwise, a decrease in efficiency apparently results because as the gelatin swells, the refractive index modulation is reduced. Although grafted-gelatin-polymer-based holograms are less sensitive to humidity at room temperature and around 50% humidity, they require effective protection against moisture at higher temperature, high humidity conditions. It was imperative that the environmental studies be divided into several subtests because the tests could not be conducted simultaneously. To the author's knowledge, this is the first attempt to evaluate holographic visible and IR filters from such a broad spectrum.

3.7.1 High Temperature Test -- No Encapsulation

High temperature stability tests were performed on selected filters with no lamination/encapsulation. The selected samples (A-F) were first conditioned at 80°C for 3 hours to remove any trace amounts of solvent and/or moisture. After conditioning, the samples were cooled to room temperature and their optical properties were determined using a spectrophotometer. All of the samples were returned to the oven and the temperature was raised according to the information in Table 3-8. For example, after 10 minutes at 100°C, Sample B was removed from the oven. After cooling to room temperature, its optical density, peak wavelength and bandwidth were measured. The procedure was repeated with an incremental increase of 20°C for each subsequent sample. A plot of the samples' spectral characteristics is shown in Figure 3-18. It can be seen from this data that an increase in temperature of up to 200°C had no significant effect on the optical density and the bandwidth of the samples. Another indication of the holographic filters' ability to survive temperature variations of up to 200°C is that there are no changes in peak height corresponding to an optical density of 4.

The high temperature stability of POC's holographic coating and/or holograms can be best explained from the chemical crosslinking and polymerization process point of view. In general, polymeric materials withstand higher temperatures compared to their corresponding monomers or oligomers. As the degree of polymerization (i.e., molecular weight) is increased, the stability is also further increased. Moreover, if the crosslinking occurs or if the number of crosslinks are intentionally increased by a chemical agent and/or processing, the temperature and other environmental stabilities are improved since the molecular packing density is enhanced. In the holographic process involving laser exposure, wet chemical processing and subsequent heating, polymerization and crosslinking occur simultaneously. As a result, holograms demonstrate extremely high temperature stability as illustrated in Figure 3-18 and Table 3-8.

Table 3-8 High Temperature Stability Study of POC's Holograms

Sample Code	Temperature °C	Time	Optical Density	Peak Wavelength λnm	Bandwidth Δλnm
A	80	3 hr.	4	590	52
B	100	10 min.	4	590	50
C	120	10 min.	4	590	49
D	140	10 min.	4	588	47
E	160	16 hr.	4	577	46
F	200	10 min.	4	577	46

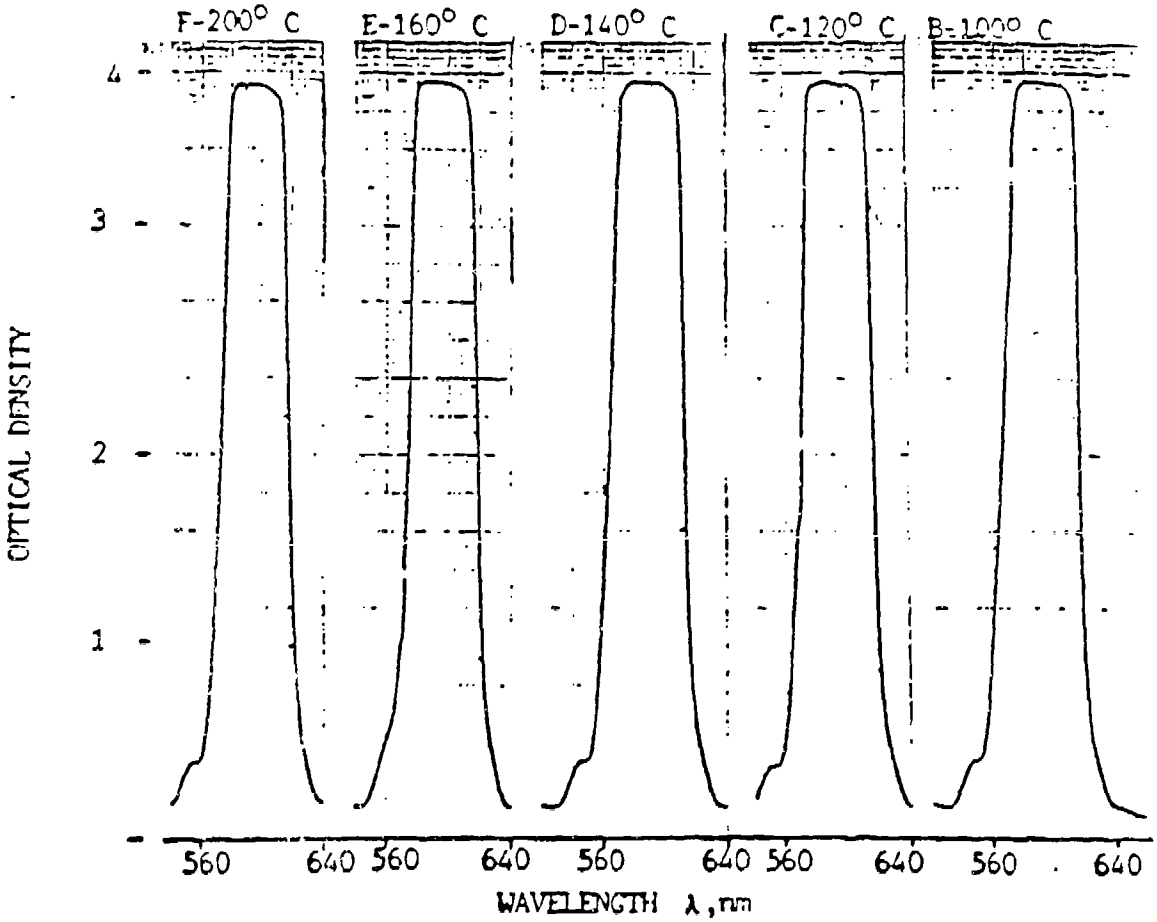

Figure 3-18 Optical density (OD) versus wavelength as a function of temperature. OD spectra were recorded on a Varian 2300 Spectrophotometer after the sample was subjected to the temperature conditions listed in Table 3-8.

3.7.2 Lamination and Encapsulation of BLEP Filters

Although RTX-2- and IRT-6-based holographic BLEP filters demonstrate temperature stability at least up to 130°C, these BLEP filters need to be protected when used in high humidity environments and/or underwater. To protect the holographic BLEP filters from moisture, POC investigated lamination and/or encapsulation of the fully-processed IR holograms. For encapsulation, an adhesive that adheres to both the recording material and the protective plate is necessary. Thus far, POC has conducted tests on several adhesives, laminating glass plates and plastics to test for the survivability of adhesives and plastic films. It was also important to determine whether the adhesive used for lamination adversely affects the IR hologram's performance. To test for this, we conducted three tests. The samples were selected from many IR filters based on their optical quality and uniformity. The samples were laminated in duplicate as described below.

1. *Underwater 52°C Temperature Test--With Encapsulation*

   For encapsulation, Samples 1-A and 2-A used Norland 68, Samples 3-A and 4-A used Master Bond UV-15-7, Samples 5-A and 6-A used Master Bond UV-15-7SP4, and Samples 7-A and 8-A used Master Bond EP-30. All samples were edge-coated with Master Bond EP-30 epoxy and baked at 52°C (125°F) for two hours prior to being immersed in water. The lamination sequence is shown in Figure 3-19. Samples were initially evaluated by UV-VIS spectroscopy, then immersed in 52°C water for 2 hours. Upon removal from the water bath, the samples were allowed to cool at room temperature for half an hour and evaluated for their change in optical characteristics (i.e., optical density, peak wavelength, and bandwidth). Bandwidth was determined as the full width at one half the maximum optical density. The water immersion cycle and the optical testing were each repeated once.

   The optical performance of the samples before and after cycles #1 and #2 is summarized in Table 3-9. The data indicate that at 52°C in underwater conditions, both the BLEP filters and the adhesives used for lamination are stable, with the exception of sample 3-A which had a 10% decrease in optical density. The rest of the samples demonstrated excellent stability and optical performance in terms of peak wavelength, bandwidth, and optical density.

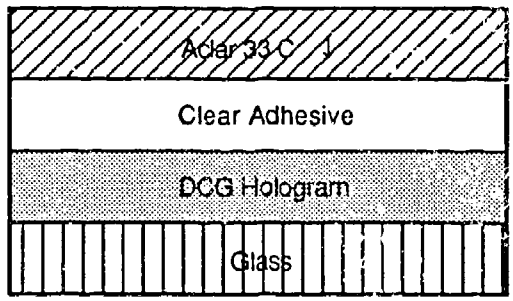

Figure 3-19 Construction of laminated DCG test samples. Aclar film was laminated with the Corona-treated surface towards the adhesive.

Table 3-9 Results of Water Immersion Tests of IR Filters

	INITIAL			1st WATER CYCLE			2nd CYCLE		
Sample #	Optical Sensitivity	Peak λ	Δλ	Optical Density	Peak λ	Δλ	Optical Density	Peak λ	Δλ
1-A	3.43	672	55	2.64	675	55	3.52	675	60
2-A	3.48	680	47	3.64	678	45	2.74	675	45
3-A	3.48	708	73	3.40	713	72	2.40	708	82
4-A	3.40	683	45	3.56	683	48	2.32	693	52
5-A	2.72	690	97	2.40	708	102	3.64	708	88
6-A	3.56	710	72	3.60	710	75	3.40	708	80
7-A	2.55	735	86	2.36	735	95	2.48	733	85
8-A	3.64	675	60	3.32	675	62	3.04	675	58

Δλ = Bandwidth

2. *Boiling Water Test--With Encapsulation*

Samples for the boiling water test were prepared using the method described above. The adhesives used were Norland 61 and Master Bond UV-15. Both adhesives cure at UV radiation (λ = 365 nm). Before lamination, the holographic filters were conditioned and the peak wavelength was stabilized. The laminated holographic filters were then subjected to the boiling water test illustrated in Figure 3-20. The boiling water test results indicate that when Norland 61 or

Master Bond UV-15 adhesives are used, there is little or no shift in peak wavelength.

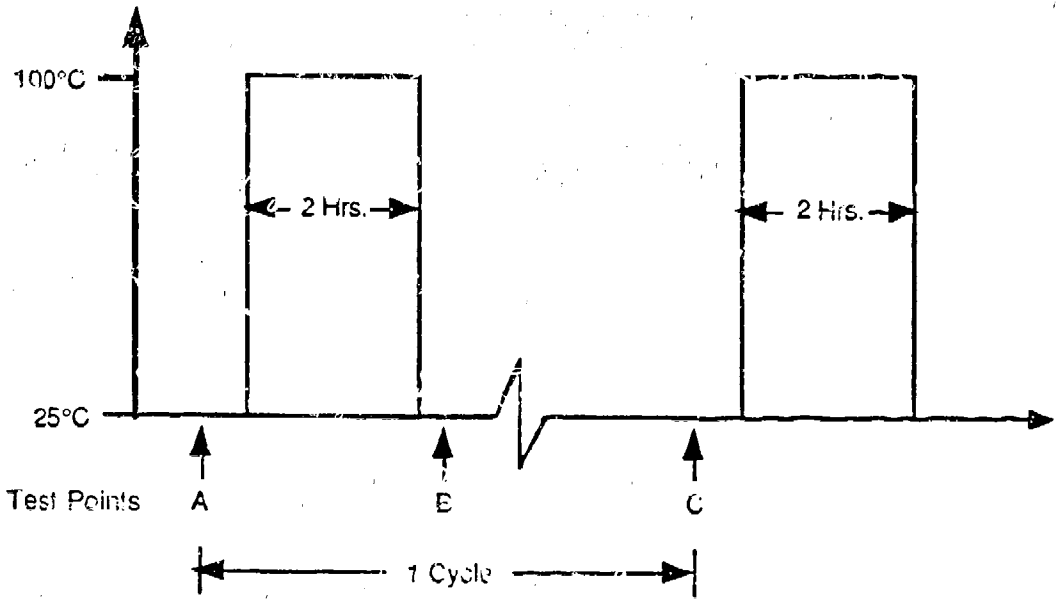

A) First Transmission Plot of Sample Under Test (S.U.T.)
B) Second Transmission Plot of S.U.T. 0.5 Hour After 2-Hour Boil Cycle
C) Third Transmission Plot of S.U.T. 48 Hours After (B)

Figure 3-20 Time Schedule for the Boiling Water Test.

3. *130°C Temperature Recycle Test--With Encapsulation*

The lamination procedure for the BLEP filters was the same as described in (1) above. After lamination and before subjecting individual samples to a 130° test cycle, the filters were tested for optical density, peak wavelength and bandwidth. These parameters were measured again after the samples were subjected to the test cycles shown in Figure 3-21. Points A, B, and C represent when the optical measurements were taken. Subjecting the samples to the bake cycles also had no significant effects on its optical characteristics.

When accelerated aging tests at temperatures above 150°C were performed on the laminated samples (Norland 61 and Master Bond UV-15), both types of samples failed to maintain their optical density. This failure may be attributed to several factors. They are:

i) There may have been trace amounts of moisture trapped between the holographic coating and the adhesive layer. At higher temperatures, these trapped water molecules aggressively penetrate the hydrophilic gelatin or graft polymer layer.

ii) Some of the reactive groups of undercured adhesive may react with the gelatin or polymer groups, thus disturbing the crosslinks that help increase material as well as refractive index modulation. Once the index modulation is disturbed, a drop in optical performance is expected.

iii) There is a chance that the curing of the adhesive may be insufficient because of a thick adhesive layer and low-power UV radiation or short curing time.

iv) The hologram processing may not be optimum.

In future experiments, we will systematically address each of the above issues by testing adhesives containing several chemical moieties which react differently with the gelatin and graft polymers used for the fabrication of the BLEP filter.

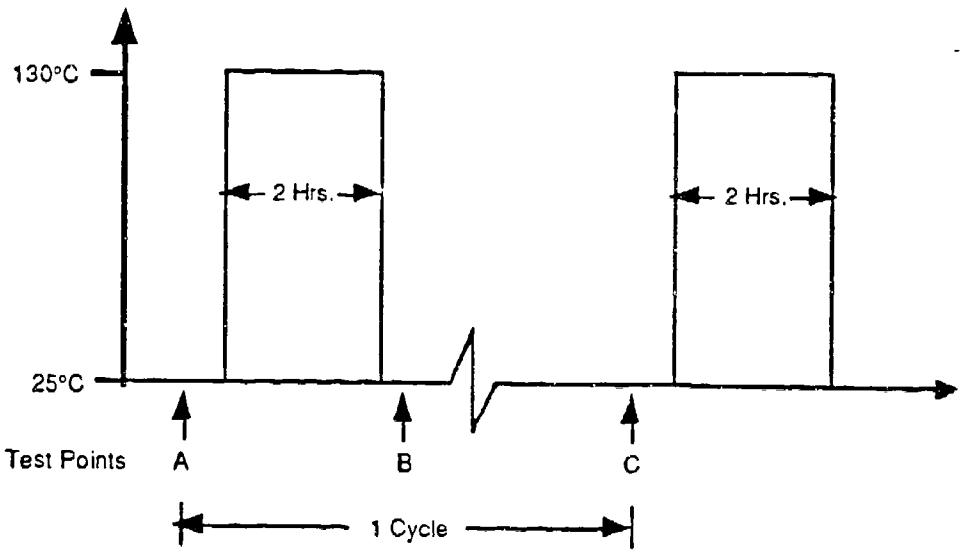

A) Transmission Plot of Sample Under Test (S.U.T.)
B) Second Transmission Plot of S.U.T. 0.5 Hour After 2-Hour Bake Cycle
C) Third Transmission Plot of S.U.T. 48 Hours After (B)

Figure 3-21 Time schedule for the high temperature cycling test.

5.0 CONCLUSIONS AND RECOMMENDATIONS

The analytical and experimental results reported in the above Sections have validated the concept of Broadband Laser Eye Protection (BLEP) filters, and demonstrated the potential effectiveness of such filters for use in protecting ground troops from eye damage by frequency agile near infrared lasers. In order to further develop the BLEP filter technology to the point in which field deployed BLEP devices can be mass produced, POC makes the following recommendations for Phase II research and development:

1. Further investigate the most critical issues related to the red sensitive material development so that a uniform broad bandwidth can be achieved. These issues will include photosensitive recording material composition involving gelatin-polymer dye and their concentration ratio.

2. Optimize exposure and processing parameters of RTX-2 and IRT-6 recording materials in order to obtain high optical density, low noise, high photopic/scotopic efficiency, and good optical uniformity in the BLEP filters.

3. Evaluate the encapsulation and lamination techniques of for protecting ELEP filters from abraison and environmental concerns so that the required ballistic protection can be accomplished. An extensive study into the compatibility of optical adhesives with the recording material and the laminating layer is necessary in order to laminate BLEP filters in a mass production environment.

4. BLEP filters need to be tested after lamination according to MIL-STD 810 for encapsulation and abrasion resistance.

5. Evaluate the optical performance of BLEP filters in harsh environmental conditions including desert temperatures for a prolonged duration. This will offer information about BLEP filter survivability. In addition, BLEP filters must be tested under other conditions including laser damage threshold, temperature recycle, long sunlight exposure, vibration, salt spray, and rain.

6. BLEP filters appear to be mass producible, however, the mass production techniques need to be further evaluated in order to make the production as cost effective as possible.

7. Mass production techniques also need to be investigated to include single and double curved substrates.

6.0 REFERENCES

1. A. Granbe, "Dye Sensitized Dichromated Gelatin for Holographic Optical Elements Fabrication," Phot. Sci. Engr. 22, 37 (1978); Opt. Commun., 8, 251 (1973).

2. M. Akagi, Phot. Sci. Eng., 18, 248 (1974).

3. T. Kubota, T. Ose, M. Sasaki, and K. Honda, "Hologram Formation with Red Light in Methylene Blue Sensitized Dichromated Gelatin," Appl. Opt., 15(2), 556 (1976).

4. R. Changkakuti, and S. Pappu, "Study of pH Dependence of Diffraction Efficiency of Phase Hologram in Dye Sensitized DCG," Appl. Opt., 25(5), 798 (1986); Appl. Opt., 27(2), 324 (1988).

5. J. Blyth, SPIE, 1212(42), 1 (1989).

6. T. P. Jannson. July 1984. "Holographic Technology," DOE Annual Report, Contract No. DE-AC03-81ER10836.

7. J. R. Magarinos, and D. J. Coleman, Opt. Engr., 24, 769 (1985).

8. J. D. Masso, "Eye Centered Interferometric Laser Protection," SPIE, March 1988.

9. J. Jannson, T. Jannson, and K. Yu, "Solar Control Tunable Lippmann Holowindow," Solar Energy Material, 14, 289 (1986).

10. E. Kogelnik, Bell Syst. Tech. J., 24, 244 (1968).

AD NUMBER

B160 619

LIMITATION CHANGES

TO Approved for Public Release; Distribution Unlimited...

— Code: A/1

FROM DoD Agencies Only..

— Code: E/4

AUTHORITY

— SGRD-RMI-S (70-1), Ft Detrick, Md, via Ltr, Gtc 4 Mar 94.

SUPPLEMENTARY

INFORMATION

DEPARTMENT OF THE ARMY
U.S. ARMY MEDICAL RESEARCH AND DEVELOPMENT COMMAND
FORT DETRICK, FREDERICK, MD 21702-5012

REPLY TO
ATTENTION OF:

4 MAR 1994

SGRD-RMI-S (70-1y)

ERRATA

MEMORANDUM FOR Administrator, Defense Technical Information Center, ATTN: DTIC-HDS/William Bush, Cameron Station, Bldg. 5, Alexandria, VA 22304-6145

SUBJECT: Request Change in Distribution Statements

1. The U.S. Army Medical Research, Development, Acquisition, and Logistics (USAMRDAL) Command (Provisional), has reexamined the need for the limited distribution statement on technical reports for Contract Nos. DAMD17-81-C-1206 and DAMD17-90-C-0086. Request the limited distribution statement for AD No. [redacted] and ADB160619, be changed to "Approved for public release; distribution unlimited," and that copies of this report be released to the National Technical Information Service.

2. The point of contact for this request is Ms. Virginia Miller, DSN 343-7328.

ERRATA -AD-B160619

CAREY O. LEVERETT
LTC, MS
Deputy Chief of Staff for
Information Management